Mixture of Sparse Attention: Content-Based Learnable Sparse Attention via Expert-Choice Routing

Piotr Piękos[1], Róbert Csordás[2], Firas Laakom[1], Nanbo Li[1], Jürgen Schmidhuber[1]

[1]**KAUST, AI Initiative, Thuwal, Saudi Arabia**
[2]**Stanford University, Stanford, CA, USA**

`piotr.piekos@kaust.edu.sa`

Reviewed on OpenReview: `https://openreview.net/forum?id=HUpBs4TZkS`

Abstract

Quadratic self-attention remains a central obstacle to scaling sequence length, but many sparse attention methods lose quality relative to dense attention under comparable compute budgets. This paper studies whether learned, content-based token selection can make sparse attention competitive with dense attention as a method for training transformer language models. We present Mixture of Sparse Attention (MoSA), an attention mechanism inspired by Mixture of Experts with expert-choice routing, where each attention head selects its own subset of tokens and computes attention only within that subset. We create a hybrid attention layer that keeps four dense heads to preserve stable dense information flow, while the remaining dense heads are replaced by a larger number of MoSA heads. Selecting k tokens from a sequence of length T reduces the per-head attention cost from $O(T^2)$ to $O(k^2 + T)$, which lets us trade each removed dense head for multiple sparse heads at matched FLOPs. In this controlled IsoFLOP setting, across dense baselines from 28M to 516M parameters, MoSA is the only tested sparse attention variant that consistently improves over dense attention, reaching up to 27% lower perplexity at the same compute budget. These results show that expert-choice, content-based sparse attention can outperform dense attention in the evaluated fixed-length, non-autoregressive training setup. We also report perplexity-matched resource measurements showing lower wall-clock time, training memory, and stored key-value pairs in our implementation, which demonstrates the potential benefits of MoSA for autoregressive models if the non-autoregressive router is adapted to causal decoding.

1 Introduction

Modern transformer architectures (Vaswani et al., 2017) have proven highly effective for sequence modeling tasks and are the key to the success of large language models (LLMs; (Brown et al., 2020; Touvron et al., 2023; Team et al., 2024; Grattafiori et al., 2024)). A key component of their success is the attention mechanism, which enables dynamic information propagation by computing weighted sums of past states for each token. This results in high computational and memory complexity, both quadratic in sequence length.

This has led the researchers to explore alternative approaches. State Space Models (Gu et al., 2020; 2022; Gu and Dao, 2023; Wang et al., 2024; Yang et al., 2025) capture long-range dependencies with just a handful of state variables rather than relying on full attention matrices. However, they fall short of full self-attention in terms of practical performance. To counteract lossy compression of State Space Models, a recent line of work investigates hybrids that combine quadratic attention and linearized memories (Park et al., 2024; Zuo et al., 2022; Lieber et al., 2024). Linear attention Katharopoulos et al. (2020); Schlag et al. (2021); Schmidhuber

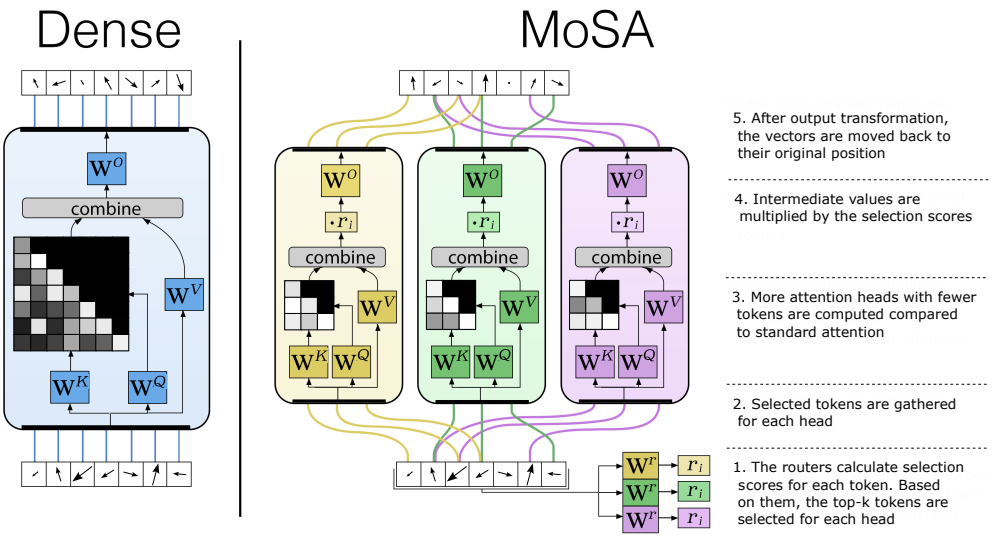

Figure 1: MoSA layer compared to the dense attention layer. MoSA replaces each dense head with multiple heads with a learnable sparsity pattern. Each head selects its own k tokens to process. MoSA calculates query, key, and value projections only for the selected token and computes the attention only between them. It drops the rest of the tokens, leading to more efficient compute utilization. This reduces the computational and memory complexity on a sequence of length T from $O(T^2)$ to $O(k^2 + T)$. The saved compute budget can be used to scale up the number of heads.

(1992)* optimizes the attention cost by changing the order of the operations in the attention after removing nonlinearity. However, it also performs poorly compared to quadratic attention (Qin et al., 2022).

As an alternative, static sparse attention methods (Child et al., 2019) reduce the quadratic complexity by selectively attending to a subset of tokens to be used in the attention. They use hand-defined coarse-grained patterns that are not data-dependent. Typical examples of these methods are the block-sparse and strided attention (Child et al., 2019; Zaheer et al., 2020; Beltagy et al., 2020). Static sparsity and block aggregation methods, however, impose significant limitations. They encourage the compression of multiple tokens into a single, lossy representation. This is necessary to remember information beyond the active block. Such compression makes fine-grained recall difficult. The problem is similar to the well-known limitation of state-space models, which are forced to compress the entire past into a fixed-size representation (Arora et al., 2024; Jelassi et al., 2024). Content-based dynamic sparse attention (Tay et al., 2021; Vyas et al., 2020; Roy et al., 2021) methods can, in principle, learn to attend to individual tokens, regardless of their location in the input, while ignoring less useful tokens. The Routing Transformer (Roy et al., 2021) clusters the tokens within each head using online K-means. However, it fails to show significant performance gains over static sparse-attention methods, possibly due to slow convergence of online K-means (Bottou and Bengio, 1994).

In this paper, we demonstrate that learned, content-based token selection can replace a significant portion of dense heads and make sparse attention competitive with dense attention as a method for training transformer language models. We propose a novel approach, inspired by Mixture-of-Experts (Shazeer et al., 2017; Fedus et al., 2022), to create a dynamic, content-based, and head-specific selection of tokens for sparse attention. This is achieved with Expert-Choice Routing (Zhou et al., 2022), where each attention head is treated like an expert and selects its own specific tokens from the input. This creates a perfectly balanced selection, avoiding the need for complicated regularization techniques. We name our approach Mixture-of-Sparse Attention(*MoSA*). Although recent work explored applying ideas from the MoE literature to attention mechanisms (Zhang et al., 2022; Csordás et al., 2024), they focus on reducing the number of materialized dense attention matrices. We propose a different approach: we make the attention matrices sparse by selecting a small subset of tokens to use for each attention head.

*Note that *unnormalized linear transformers* (with "linear attention") were first published in 1992 under the name *fast weight controllers* (Schmidhuber, 1992) or *fast weight programmers*.

By selecting k tokens from a sequence of length T, MoSA reduces the computational complexity of each attention head from $O(T^2)$ to $O(k^2 + T)$. Sparse attention techniques have historically been employed out of necessity to manage long sequences that exceed available computational capacities. In contrast, we also explore the use of the saved computation budget for creating additional attention heads. In our main experiments, we use this idea in hybrid attention layers that retain four dense heads and replace the remaining dense heads with a larger number of highly sparse MoSA heads. This setup encourages sparse-head specialization while preserving a small dense pathway for stable information flow. We show that this allows for better utilization of the available compute budget and leads to substantially better iso-flop language modeling performance compared to dense attention. Furthermore, we analyze other sparse attention methods, such as fixed sparse attention (Child et al., 2019) and the Routing Attention (the attention introduced in the Routing Transformer) (Roy et al., 2021). MoSA is the only sparse attention method we analyzed that consistently demonstrates improvement over dense baselines across all model scales in the IsoFLOP setting.

Our main results demonstrate that hybrid models with four dense heads and many MoSA heads significantly improve the model's quality by up to 27% in an IsoFLOP setting. Specifically, we evaluate MoSA on a language modeling task by starting with dense baselines and incrementally sparsifying the attention. We ensure FLOP-matching by swapping a specific number of dense heads for *more* sparse heads. We repeat this procedure on different scales, starting with baselines from 28M to 516M parameters. MoSA consistently improves perplexity across all model scales.

The IsoFLOP results demonstrate MoSA's superior performance in a FLOP-matched setting. We additionally study a perplexity-matched setting to understand the resource profile of MoSA beyond idealized FLOP counts. In our implementation, MoSA exhibits improved wall-clock time and GPU memory consumption even without a specialized CUDA kernel, and it reduces the total number of keys and values used in the computation. Since KV-cache size is an important practical problem for autoregressive LLM inference and is the main focus of many post-training sparse attention methods (Liu et al., 2023; Li et al., 2025; Cai et al., 2024), these measurements demonstrate the potential practical benefits of MoSA if its adapted to causal decoding. We report these measurements in Section 3.2.

In summary, our contributions are the following:

1. We propose MoSA, a sparse attention method that uses a *learned*, context-based token selection, with each of the heads attending to a small subset of all tokens.
2. We evaluate hybrid MoSA in an IsoFLOP setting on four different scales with dense baselines ranging from 28M parameters to 516M. In this setting, hybrid MoSA improves perplexity by up to 27%. MoSA is the only sparse attention method we analyzed that consistently improved perplexity compared to the dense baseline across all model scales.
3. We demonstrate that, in a perplexity-matched setting, a pure PyTorch implementation of MoSA improves both wall-clock time and memory usage simultaneously, without requiring specialized fast kernels. This setup also reduces the number of stored keys and values, suggesting potential KV-cache savings for future autoregressive adaptations of MoSA.
4. We demonstrate that on long sequences, MoSA maintains a large advantage compared to other tested sparse-attention methods.

The paper is organized as follows. Section 2 provides the necessary background and describes MoSA. Section 3 includes the experimental setup and the results. Section 4 discusses related work, and Section 5 provides a general discussion as well as potential future directions.

2 Method

2.1 Background

Here, we will discuss the necessary background on multi-head self-attention and mixtures of experts, which are required to understand our method.

Attention Mechanism. Attention assigns input-dependent weights to tokens in a sequence, allowing each token to gather context from the rest of the sequence. To do this, each token is projected to three vectors: its *query*, *key*, and *value*. For a given token, we compare its *query* vector with the *key* vectors of all tokens (including itself), producing a set of similarity scores. The scores are then normalized and used to calculate a weighted sum of the tokens' *value* vectors. The result is a new representation that dynamically integrates information throughout the sequence.

Let T be the sequence length, h the hidden dimension of the model, and h' the hidden dimension in each head. $\mathbf{Q}, \mathbf{K}, \mathbf{V} \in \mathbb{R}^{T \times h'}$ represent the query, key and value matrices, respectively.

The attention output is computed as:

$$\text{Attention}(\mathbf{Q}, \mathbf{K}, \mathbf{V}, \mathbf{M}) = \text{softmax}\left(\frac{\mathbf{Q}\mathbf{K}^\top + \mathbf{M}}{\sqrt{h'}}\right)\mathbf{V} \tag{1}$$

Here, $\mathbf{M}$ denotes the attention mask that represents hard modeling constraints. $\mathbf{M}_{i,j} = 0$ if and only if $i - th$ token is allowed to attend to $j - th$ token, otherwise $\mathbf{M}_{i,j} = -\infty$. In causal language models, $\mathbf{M}_{i,j} = 0 \iff i \geq j$ ensures that no token can attend to the future.

The multi-head attention (MHA) creates multiple instances of query, key, and value matrices from an input sequence $\mathbf{X} \in \mathbb{R}^{T \times h}$ and applies the attention to each instance independently. These instances are called heads. Each head has its own mappings $\mathbf{W}_i^Q, \mathbf{W}_i^K, \mathbf{W}_i^V \in \mathbb{R}^{h \times h'}$ and $\mathbf{W}_i^O \in \mathbb{R}^{h' \times h}$, where $i \in \{1..H\}$ and H is the number of heads. h' is typically set to $\frac{h}{H}$. $\mathbf{Q}_i = \mathbf{X}\mathbf{W}_i^Q, \mathbf{K}_i = \mathbf{X}\mathbf{W}_i^K, \mathbf{V}_i = \mathbf{X}\mathbf{W}_i^V$.

$$\mathbf{X}_{out} = \sum_{i=1}^{H} \text{Attention}(\mathbf{Q}_i, \mathbf{K}_i, \mathbf{V}_i, \mathbf{M})\mathbf{W}_i^O \tag{2}$$

The resulting mechanism allows the model to adaptively focus on relevant information while maintaining differentiability. The lack of recurrence in the operations enables parallel processing of sequence elements. However, $\mathbf{Q}\mathbf{K}^\top$ is a $T \times T$ matrix and therefore introduces quadratic computational and memory complexity as a function of the sequence length.

Mixture of Experts. Mixture of Experts (MoE) combines multiple specialized neural networks (experts) with a gating mechanism that learns to route each input to the best-matching experts, activating only a small subset of experts per example. An MoE layer then computes its output as a sparsely weighted combination of the predictions of selected experts, with routing weights dynamically determined by the gating network.

Formally, given an input $\boldsymbol{x} \in \mathbb{R}^h$, the MoE layer with E experts and a scoring function (a router) $sel : \mathbb{R}^h \to \mathbb{R}^n$ can be expressed as $y(\boldsymbol{x}) = \sum_{i \in \mathcal{E}} r_i(\boldsymbol{x}) E_i(\boldsymbol{x})$ where $y(\boldsymbol{x})$ is the final output of the layer and $E_i(\boldsymbol{x})$ is the output of the expert i. $\mathcal{E}$ is the set of selected experts, usually defined as $\mathcal{E} = \text{argtopk}(r(\boldsymbol{x}) + \varepsilon, k)$, where $k \in \mathbb{N}$ is the number of active experts, ε is a stochastic noise present only during the training for exploration. The inputs are processed only by the active experts.

A critical challenge in MoE routing is ensuring balanced expert utilization. Without explicit constraints, the routing mechanism tends to overutilize a few experts while leaving others inactive. This phenomenon, known as the load-balancing problem (Shazeer et al., 2017), can significantly limit the model's capacity and effective number of parameters. Traditional approaches address this through auxiliary load-balancing losses (Lepikhin et al., 2021; Fedus et al., 2022) that encourage uniform expert utilization across a batch of inputs.

In contrast, Expert-Choice routing (Zhou et al., 2022) ensures perfect load balancing by inverting the traditional routing paradigm. Instead of the tokens choosing their experts, the experts choose which inputs they prefer to process. Given a batch of B inputs, each expert selects the top-k out of the B inputs it will process.[†]

Similarly to token choice routing, expert choice also reduces the *average* number of experts used to process a token. However, in contrast to token-choice routing, the amount of compute assigned is *different* between

[†]In our case, each expert selects top-k tokens from the sentence to process independently for each batch.

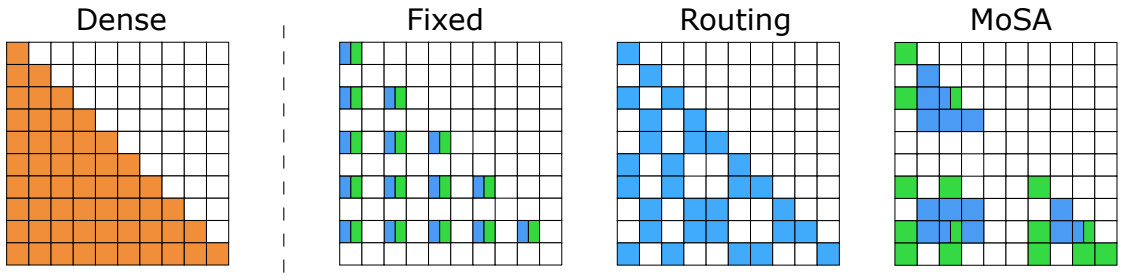

Figure 2: Attention variants visualized. In the plot, the colors indicate different heads. Sparse attention methods are roughly FLOP-matched and have sparsity $\rho = 2$. One Routing Attention head corresponds in FLOP-cost to ρ Fixed/MoSA heads. Fixed sparse attention uses only $k = \frac{T}{\rho}$ tokens in specific positions, with regular stride. The Routing Attention clusters tokens within each head into ρ clusters of size k based on their representations. MoSA selects k tokens for each attention head independently based on their representations.

tokens. This can be beneficial, as some tokens might be harder than others and therefore should benefit from more compute. On the other hand, it might lead to uneven resource allocation, where some tokens are assigned disproportionately high compute while others might starve.

Traditionally, Mixture of Experts has been applied in transformers as a replacement for a feedforward block, which is the most parameter-heavy part of the model. However, MoEs are sometimes also applied to the attention layer. SwitchHead (Csordás et al., 2024) reduces the total number of heads by replacing some of the transformations with MoEs inside the attention. MoA (Zhang et al., 2022) enhances Multi-Query Attention (Shazeer, 2019) by adaptively selecting query transformations for each token. Similarly to these, we also apply the MoE to the attention layer, but in a way that introduces sparsity in the attention mechanism.

2.2 Mixture of Sparse Attention (MoSA)

Sparse attention methods model global dependencies by selecting specific tokens that can attend to other specific tokens based on a hand-engineered set of rules (Beltagy et al., 2020; Zaheer et al., 2020) or by blockwise aggregation of tokens (Yuan et al., 2025). Both of these families of methods impose the mixing of information during token aggregation, either explicitly or implicitly.

We propose instead to select tokens adaptively for each head based on the input. Thus, a flexible set of important tokens can be kept around, creating content-based sparsity without the need for information mixing. To achieve that, we take inspiration from Expert-Choice routing in MoEs. We name our method *Mixture of Sparse Attention (MoSA)*. MoSA learns which individual tokens to use for attention through end-to-end training. Each attention head in MoSA learns its own unique sparsity pattern, allowing different heads to specialize in different subsets of tokens relevant to their particular function within the network. This diverse, head-specific token selection pattern ensures that the model preserves the granular information within each relevant token while dynamically discovering optimal sparsity patterns specific to the data distribution. The architectural difference between MoSA and dense attention is illustrated in Fig. 1.

The sparsity in MoSA reduces the computational cost of each attention head, allowing the use of more heads to develop targeted projections optimized for specific relationship types. The computational savings are particularly substantial when the number of selected tokens is significantly smaller than the sequence length.

In MoSA, in addition to the standard projections, each head has an additional router that selects which tokens are used for that head. Formally, the router is defined using the weight matrix $\mathbf{W}^r \in \mathbb{R}^h$. Let $\mathbf{X} \in \mathbb{R}^{T \times h}$ be the T-long sequence of input tokens. The router calculates the selection scores for each token $\mathbf{r} = \sigma(\mathbf{X}\mathbf{W}^r) \in \mathbb{R}^T$. For σ we use the non-competitive sigmoid function $\sigma(x) = \frac{1}{1+e^{-x}}$ following observations from σ-MoE (Csordás et al., 2023). Subsequently, we use expert choice for the selection of tokens for each head:

$$\mathbf{r}^{topk}, I = TopK(\mathbf{r}, k)$$

where $TopK$ returns the highest k values of $\boldsymbol{r}$ called $\mathbf{r}^{topk} \in \mathbb{R}^k$, along with their indices $I \in \{0, ..., T-1\}^k$. I is used to select the subset of inputs for the MoSA head:

$$\mathbf{X}^s = (\mathbf{X}_{I_1}, \mathbf{X}_{I_2}, ..., \mathbf{X}_{I_k}) \in \mathbb{R}^{k \times h}$$

where $\mathbf{X}_i$ represents $i-th$ row from matrix $\mathbf{X}$. After that, queries, keys, and values are calculated identically to the standard MHA: $\mathbf{X}^s$ as $\mathbf{Q} = \mathbf{X}^s\mathbf{W}^Q, \mathbf{K} = \mathbf{X}^s\mathbf{W}^K, \mathbf{V} = \mathbf{X}^s\mathbf{W}^V$. As our primary target is language modeling, we also calculate the mask that prohibits attending to future tokens. Unlike the standard MHA, this mask is not triangular and has to take into account the token indices selected by the head: $\mathbf{M}_{i,j} = 0 \iff I_i \geq I_j, -\infty$ otherwise.

The sparse attention can be computed using the standard attention defined in Eq. 1. $\mathbf{A} = \text{Attention}(\mathbf{Q}, \mathbf{K}, \mathbf{V}, \mathbf{M})$. This allows the combination of MoSA with optimized attention implementations such as Flash Attention (Dao et al., 2022). The resulting vectors $\mathbf{A}_i$ are multiplied by the corresponding router values $\mathbf{r}_i$. Then, after the output transformation $\mathbf{W}^o$, they are moved back to their original positions in the full-length sequence $\mathbf{Y} \in \mathbb{R}^{T \times h}$.

$$\mathbf{X}^o = \text{diag}(\mathbf{r})\mathbf{A}\mathbf{W}^o \in \mathbb{R}^{k \times h}$$
$$\mathbf{Y}_j = \begin{cases} \mathbf{X}^o_i, & \text{if } j = I_i \text{ for some } i \in \{1, \ldots, k\}, \\ 0, & \text{otherwise,} \end{cases} \quad \text{for } j = 1, \ldots, T.$$

$\text{diag}(\cdot)$ creates a diagonal matrix from a vector, used for elementwise scaling of the columns of the matrix $\mathbf{A}$ by a vector $\mathbf{r}$. This ensures that the token's contribution is proportional to the router's output. This also enables the router to receive gradients, making it learnable by gradient descent.

We call the combined transformation of x into y, parameterized by $\theta_i = (\mathbf{W}^Q, \mathbf{W}^K, \mathbf{W}^V, \mathbf{W}^O, \mathbf{W}^r)$ a single MoSA head: $\mathbf{Y} = \text{MoSA}_{head}(\mathbf{X}; \theta_i)$. A MoSA layer parameterized by $\theta = \{\theta_i\}_{i \in 1 \ldots H}$ is a sum of all MoSA heads

$$\text{MoSA}(\mathbf{X}; \theta) = \sum_{i=1}^{H} \text{MoSA}_{head}(\mathbf{X}; \theta_i) \tag{3}$$

The entire transformation in the multihead version can be efficiently implemented in PyTorch (Paszke et al., 2019) using `einsum`, `scatter` and `gather` operations.

Hybridization. Sparse attention methods are usually combined with local attention (Child et al., 2019; Roy et al., 2021) when used on long sequences. Sparse attention then captures global dependencies, while local attention preserves local context. As our setup permits the use of dense attention, in our main experiments, we combine MoSA or corresponding sparse attention baseline with 4 dense heads. In Appendix C, we demonstrate the necessity of hybridization and motivate our selection of four dense heads for the models. In Section 3.3, we combine MoSA with local attention for long sequences and demonstrate that MoSA demonstrates superior performance in this scenario as well.

Positional encodings. All our experiments use Rotary Positional Encodings (RoPE) (Su et al., 2021). RoPE applies positional encodings for each attention head after query and key mapping. It does this by rotating them at an angle determined by the token's position in a sentence. Similarly to the attention mask, we must ensure that the rotations correspond to the token's original position in the sequence $\mathbf{X}$ rather than the selected subset $\boldsymbol{X}^S$. Thus, we adapt RoPE to be aware of token positions I. Following standard practice, we rotate half of the dimensions and leave the other half unchanged.

3 Experiments

In this section, we empirically demonstrate MoSA's performance in different settings. We compare MoSA to dense and sparse baselines introduced in Section A. In Section 3.1, we evaluate all the methods on language modeling under a fixed FLOP budget. In Section 3.2 we demonstrate the practical benefits of MoSA by

#Params Dense	Tiny 28M	Small 113M	Medium 210M	Large 516M
Dense	22.46	16.01	13.95	12.20
Fixed	23.28	16.51	14.35	12.40
Routing	23.33	16.43	14.21	12.24
MoA	21.33	15.87	14.09	12.30
NSA	22.38	15.99	13.93	12.27
MoSA(ours)	**16.39** (−27.0%)	**12.85** (−19.7%)	**11.06** (−20.7%)	**10.58** (−13.3%)

Table 1: Comparing perplexity ↓ of MoSA and baselines under a fixed computational budget (see Section 3.1). For sparse models, the table contains the best perplexity across all sparsities greater than 1. The results for sparse models were selected as the best of all sparsities. Relative difference to the dense baseline is displayed in the parentheses. MoSA significantly outperforms the dense baseline, reducing perplexity by up to 27%. The fixed and the Routing Transformer baselines both fail to reach the performance of the dense model.

measuring wall-clock time, memory usage, and KV cache size in a perplexity-matched setup. In Section 3.3 we investigate the performance of MoSA on long sequences.

We use four model sizes for our experiments: *Tiny*, *Small*, *Medium* and *Large*. Each size is defined by the *FLOP count* of the forward pass of the corresponding dense transformer baseline. The parameter count of the dense model for each size is: 28M for *Tiny*, 113M for *Small*, 210M for *Medium*, and 516M for *Large*.

Implementation details We use the SentencePiece (Kudo and Richardson, 2018) tokenizer based on sub-word units (Sennrich et al., 2016; Schuster and Nakajima, 2012) with a vocabulary size of 8000. All our models are trained on the C4 (Raffel et al., 2020) dataset for 100k batches, with batch size $B = 64$ and sequence length $T = 1024$. This means that we train on the $10^5 SB \approx 6.5B$ tokens from the dataset. We use the Adam (Kingma and Ba, 2015) optimizer with a learning rate of 0.00025, gradient clipping above the norm of 0.25, and a linear warmup for 4k steps. For detailed hyperparameters, please refer to Appendix G.

3.1 Main Results

To evaluate sparse methods, we evaluate multiple models with a gradually increasing sparsity rate $\rho = \frac{T}{k}$. This reduces the compute requirements for each sparse head. We use the saved budget to increase the number of sparse heads. Specifically, we choose the number of sparse heads to be the maximum such that the FLOPs of the sparse model do not exceed the FLOPs of the baseline model for a given size. All sparse models include four dense heads that we keep (see Section 2.2), and are included in the FLOP calculations.

Note that increasing the number of attention heads also increases the memory requirements of all methods. Consequently, for the larger FLOP-matched models, we restricted the explored sparsity values to ensure that the models fit in the memory budget dictated by our hardware.

In the IsoFLOP experiments, following observations from StreamingLLM (Xiao et al., 2024) on the importance of first tokens in the attention mechanism, we always include the first token in all MoSA heads. The head selects $k - 1$ tokens based on their router scores and the first token. The representation of the first token, just like the others, is multiplied by its router score after the attention mechanism.

IsoFLOP Curves. Starting from sparsity 1, which corresponds to the dense model, we gradually increase sparsity and measure the test-set perplexity of FLOP-matched models. Table 1 lists the best results for each model class and size. Across all model sizes, MoSA achieved significantly better perplexity within fixed FLOP

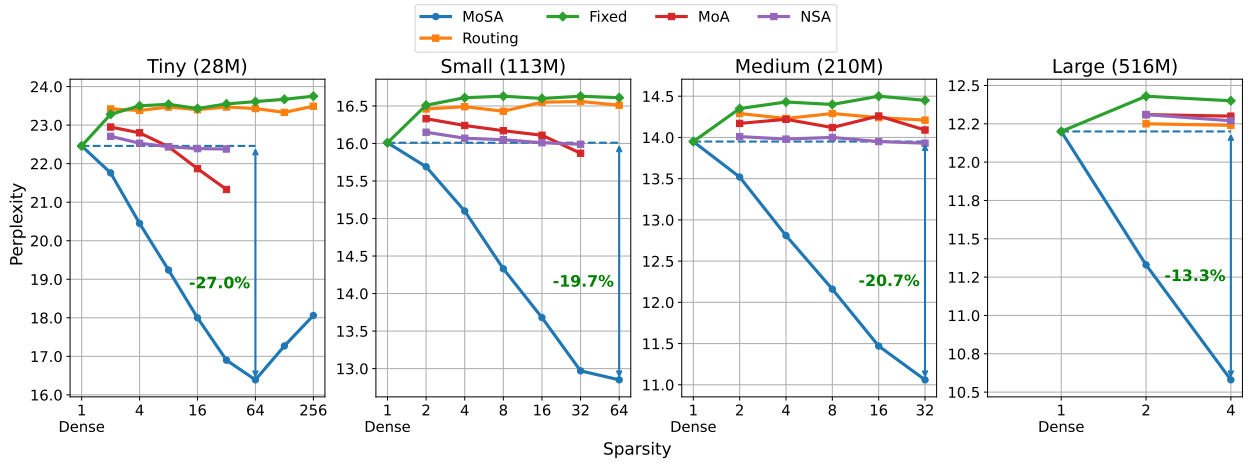

Figure 3: Perplexity (↓) of FLOP matched models under different sparsities. Each plot corresponds to a specified FLOP budget per step. The number in parenthesis is the number of parameters of the dense baseline. Sparsity 1 represents the dense baseline. As sparsity increases, MoSA's perplexity improves monotonically until saturating around sparsity 32-64, beyond which performance deteriorates. This is likely because at very high sparsity levels, each attention head selects only a few tokens, which is insufficient to capture complex relations. On the other hand, other sparse methods fail to reach the perplexity of the dense baseline in the IsoFLOP setting. We explore fewer sparsity levels for larger models due to excessive memory requirements.

budgets compared to dense baselines. All MoSA hybrids reduce the baseline's perplexity, sometimes by 27%. On the other hand, the sparse baselines for all sparsities $\rho > 1$ perform worse than the dense baseline.

Figure 3 illustrates the IsoFLOP curves of the models with varying degrees of sparsity. For MoSA, performance steadily improves as sparsity increases, reaching optimal results at approximately $\rho = 64$. Beyond this threshold, performance begins to decline, creating a "U" shape in the curve. This is likely because the excessively high sparsity values limit the model's ability to capture complex attention patterns. For example, at $\rho = 256$ with a sequence length of $T = 1024$, only $k = 4$ tokens participate in each attention head.

For some configurations, MoSA proves to be more efficient than the dense model even in a parameter-matched setting. For example, *Medium* model with sparsity 8 has $442M$ parameters and perplexity 12.16, while the *Large* baseline model has $516M$ parameters and perplexity 12.20. This shows that a higher specialization of the heads might lead to improved performance even when we discard computational benefits. Detailed results for different MoSA sparsity configurations, together with the total number of parameters and the number of heads, are listed in Table 7.

In contrast to MoSA, both fixed sparse attention and the Routing Attention consistently underperform the dense baseline across all sparsity levels. They exhibit relatively constant, but worse, perplexity across different sparsity values, with only minor fluctuations that reveal no discernible trend.

3.2 Resource Optimization

The previous section shows MoSA's ability to achieve better perplexity than dense transformers with an identical compute budget. In this section, we examine MoSA's practical efficiency gains. Specifically, we match the perplexity of MoSA and the dense baseline to measure wall-clock time, memory, and KV-cache savings.

To find the perplexity-matched comparison, we select sparsity to be equal to 32 for model sizes *Tiny, Small* and *Medium*. For *Large* we select $\rho = 16$ to keep sparsity closer to the range investigated in Section 3.1. Then, we gradually increase the number of MoSA heads until the perplexity matches the dense baseline. We do it for all four model scales defined in Section 3.1.

The results are shown in Table 2. MoSA can match the dense baseline, while being faster in wall-clock time and using less memory at the same time. These findings show that MoSA not only improves model quality in the FLOP-matched setting but can also be used to reduce computational and memory requirements when targeting the same performance level. Furthermore, it shows that MoSA uses computation more effectively than standard dense attention across all efficiency metrics.

MoSA achieves this without a specialized CUDA kernel using only PyTorch-level operations. We expect that designing a specialized kernel would result in additional significant efficiency gains.

In addition to the speed and memory used for the training, we report the total number of key-value pairs (KV) used, calculated as $\text{KV} = TH_{dense} + kH_{mosa}$, where H_{dense} and H_{mosa} represent the number of dense and sparse heads, respectively. KV directly corresponds to the size of the costly KV-Cache in the autoregressive setting. KV cache optimization has been the goal of many post-training sparse-attention methods (Liu et al., 2023; Li et al., 2025; Cai et al., 2024). Our results demonstrate that MoSA offers a significant reduction in KV-cache size while simultaneously improving speed and memory requirements.

	Tiny		Small		Medium		Large	
	Dense	MoSA	Dense	MoSA	Dense	MoSA	Dense	MoSA
Dense Heads	9	4	9	4	9	4	16	4
MoSA Heads	0	17	0	14	0	12	0	16
Perplexity (↓)	22.46	22.40	16.02	16.01	13.94	13.76	12.20	12.16
Wall-time/step ↓ (ms)	137	**127**	326	**319**	619	**592**	807	**703**
Wall-time/step gain (%)	–	−7.3%	–	−2.1%	–	−4.4%	–	−12.9%
Memory ↓ (GB)	21.1	**19.0**	32.4	**31.4**	50.2	**49.4**	104.1	**94.5**
Memory gain (%)	–	−10.0%	–	−3.1%	–	−1.6%	–	−9.2%
KV Total ↓ (K)	9.2	**4.5**	9.2	**4.4**	9.2	**4.4**	16.4	**5.0**
KV Total gain (%)	–	−51.1%	–	−52.2%	–	−52.2%	–	−69.5%

Table 2: Resource usage reduction from perplexity-matched MoSA models. KV is the KV-cache size, representing the total number of key-value pairs required (in thousands). MoSA models match the perplexity of dense baselines while at the same time improving wall-clock time, using less memory, and significantly smaller KV cache for all model sizes. Resource usage was measured on a single A100 GPU for *Tiny, Small* and *Medium* models and on two A100 GPUs for *Large*.

3.3 Scaling with Sequence Length

Traditionally, sparse attention methods have been introduced as a necessity when sequence length makes dense attention computationally prohibitive. After demonstrating MoSA's effectiveness in standard-length sequences, we now investigate whether MoSA's benefits are retained or amplified in this long sequence setup.

In contrast to previous sections, here we combine MoSA or a baseline method with local attention (Child et al., 2019; Beltagy et al., 2020). We use local attention instead of dense attention because even a small number of dense attention heads would result in prohibitive memory usage in a longer context scenario. This is a standard practice in the sparse attention literature (Child et al., 2019; Roy et al., 2021). Local attention preserves local dependencies, while global, sparse attention enables efficient processing of long dependencies.

We scale our sequence length from 1024 to 8196 tokens and keep the k constant equal to 64. Hence, the sparsity increases from $\rho = 16$ for $T = 1024$ to $\rho = 128$ for $T = 8192$. Contemporary sparse attention methods for long sequences are trained in longer sequences (Yuan et al., 2025). However, due to our limited hardware budget, we restrict our experiments to a sequence length of 8192. We treat this investigation as a preliminary analysis that demonstrates the potential of MoSA for long sequences. Importantly, it demonstrates that MoSA performs well when combined with local attention, which is a typical long-sequence setup.

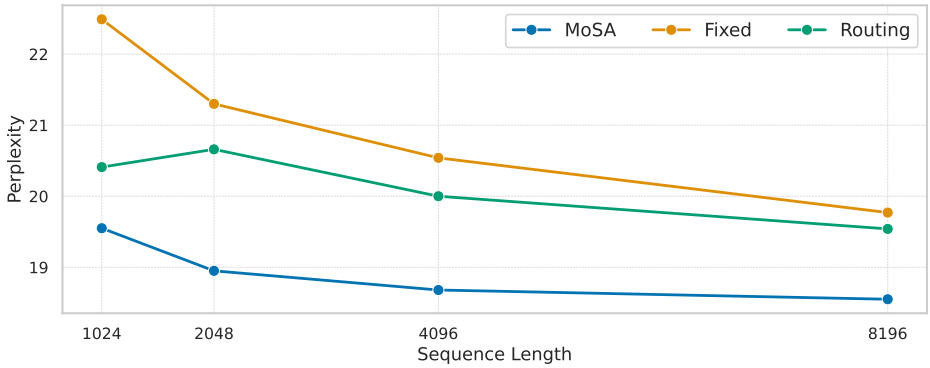

Figure 4: Perplexity of sparse-attention methods (MoSA, Fixed, and Routing) as sequence length increases. Each method has a fixed size window size (cluster size for the Routing Transformer, number of tokens selected for each head in MoSA and Fixed) regardless of total sequence length. MoSA matches the computational cost of the fixed sparsity baseline while requiring fewer FLOPs than the Routing Attention and consistently achieves the lowest perplexity.

As in the previous section, we compare MoSA with fixed sparse attention and the Routing Attention. All long sequence models have 6 layers and hidden dimension size of 1024. The Routing Transformer has 4 local attention heads and 4 Routing Transformer heads in all layers, whereas the fixed sparse attention and MoSA have 60 sparse heads and 4 local attention heads. We chose 60 sparse heads to roughly FLOP match all models for $T = 1024$. However, as we keep k constant, for longer sequences with $2048, 4096$ and 8192 tokens, the FLOP cost for fixed attention and MoSA will be much lower than for the Routing Attention. For $T = 8192$ FLOP cost of 60 MoSA's heads is equal to only 22.99% of 4 Routing Transformer heads.

The results are shown in Fig. 4. MoSA significantly outperforms other sparse attention methods across all sequence lengths. This is true even at length 8192, where MoSA uses only a small fraction of the computational cost of the Routing Transformer.

The significant performance gap in the results demonstrates the potential of MoSA for ultra-long sequences (Kitaev et al., 2020; Yuan et al., 2025; Xu et al., 2025). Given our limited resources, we leave the investigation of MoSA in this context for future work.

4 Related Work

The quadratic cost of attention in the 2017 transformer model (Vaswani et al., 2017) has led to a wide body of research on efficient attention variants (Kitaev et al., 2020; Choromanski et al., 2021). Popular alternatives are different linear attention variants that typically use a fixed vector or matrix memory and update it recurrently. The 1992 unnormalised linear Transformers (Schmidhuber, 1992; Katharopoulos et al., 2020; Schlag et al., 2021) trade performance for better computational efficiency. State space models (Gu et al., 2020; 2022; Gu and Dao, 2023) are popular alternatives that offer efficient, parallel training while keeping linear cost and efficient inference. The parallel training requirement forces only a linear recurrent relation between the timesteps. A common characteristic of such models is the relatively small, fixed memory that requires extreme compression. Despite recent progress, these models still underperform quadratic attention on many benchmarks (Arora et al., 2024; Jelassi et al., 2024).

Sparse attention methods aim to mitigate the quadratic cost of full attention by computing attention scores for only a subset of token pairs rather than the full attention matrix. These methods typically employ various heuristics to strategically identify which tokens and token relationships are the most important to process. This is often done by introducing special tokens that serve as higher-level representations of entire chunks of tokens, or by assuming emergent hierarchical structures within the attention patterns. For example, SepLLM (Chen et al., 2024) uses separators in the sentence as special tokens that sparse attention focuses on. Sparse Transformer (Child et al., 2019) uses static attention patterns to reduce computational complexity.

Longformer (Beltagy et al., 2020) combines sliding window attention with additionally selected tokens globally available. BigBird (Zaheer et al., 2020) combines sliding window attention and global attention on selected tokens, while additionally including randomly selected tokens in the attention. Streaming LLM (Xiao et al., 2024) discovers and preserves attention sinks as a necessary component despite their inefficiency and combines them with sliding window attention. Some methods (Liu et al., 2023; Li et al., 2025; Cai et al., 2024) focus on post-training attention reduction, motivated by KV-cache reduction. Hash Attention (Desai et al., 2024) uses top-k selection in the attention scores to induce sparsity and improve efficiency. However, learnable sparse attention that can also be used during training (Yuan et al., 2025) remains important as the quadratic cost of the self-attention mechanism is also problematic in the very costly pretraining phase.

Mixture-of-Experts (MoE) (Shazeer et al., 2017) have emerged as a promising paradigm for scaling model capacity without a proportional increase in computational cost. By adaptively routing input tokens to specialized experts, MoE architectures selectively activate only a part of the network. MoEs applied to transformer feedforward networks (Lepikhin et al., 2021; Fedus et al., 2022) have been widely adapted in LLMs (Guo et al., 2025; Jiang et al., 2024; Shen et al., 2024a).

A crucial challenge in MoE is to learn a balanced routing, so that experts are utilized uniformly. Imbalanced routing leads to capacity bottlenecks when certain experts become overused while others are completely ignored. This phenomenon is called expert collapse (Shazeer et al., 2017). Most approaches mitigate it by specific losses that penalize polarized expert selection (Lepikhin et al., 2021), while others propose alternative routing methods (Lewis et al., 2021; Roller et al., 2021). Expert-Choice routing (Zhou et al., 2022) inverts the selection problem, allowing each expert to choose its preferred tokens. This way, Expert-Choice routing achieves perfect load balancing by definition, at the cost that some tokens are ignored and some are overutilized. Expert-Choice routing, however, cannot be directly applied to autoregressive modeling as it uses a non-autoregressive top-k operation over the tokens. MoD (Raposo et al., 2024) proposes methods to transfer nonautoregressive expert choice routing to an autoregressive model. We leave the investigation of their adaptation to MoSA for future work.

MoE is most often applied to the feedforward part of the transformer. In contrast, some works explore MoEs in the attention mechanism to reduce the high computational cost and memory. Mixture-of-Attention Heads (MoA) (Zhang et al., 2022) selects k query transformations for each token and shares a single key and value projections similarly to Multi-Query Attention (MQA) (Shazeer, 2019). MoA allows for increasing the total number of query heads when using MQA without significantly increasing the computational cost. In contrast, MoSA selects tokens that are routed to full heads with separate queries, keys, and values (and consequently, outputs) utilizing perfect load balancing from expert choice routing for efficient sparse attention. This reduces the cost of each attention head significantly more than MoA and does not require MQA (although it might be combined for further benefits, which we leave for future work). Moreover, MoSA allows for KV-cache savings by reducing the number of selected keys, which is not possible with MoA, apart from the MQA benefit of having single KV transformations. SwitchHead (Csordás et al., 2024) reduces the number of heads (and therefore the number of computed attention matrices) by adding internal experts that can compensate for the lower number of heads. This is orthogonal to MoSA and possibly can be combined for further improvements. Multi-head attention as Mixture of Head Attention (Jin et al., 2024) proposes to use dynamic weights for the output projection in order to treat the heads as experts for tokens. However, it requires calculating all attention matrices, lacking the benefits of sparse computation.

Mixture-of-Depths(MoD) (Raposo et al., 2024) selects inputs to pass through a given entire transformer block to allow adaptive computation. This includes the attention mechanism. This produces efficiency gains in an FLOP-limited budget for the entire training. MoSA has multiple selection mechanisms, one for each head, and by increasing the number of heads it processes the sentence in a distributed way - each head processing its own chunk of the sentence.

5 Limitations and Future work

The main limitation of the current MoSA formulation is that expert-choice routing selects the top-k tokens after observing the full sequence. Consequently, the experiments in this paper evaluate MoSA as a method for fixed-length, non-autoregressive training, and the reported KV-cache reduction should be interpreted as a

property that could benefit autoregressive inference only after a causal adaptation is introduced. Possible adaptations include MoD-style post-training classifiers, natively causal token-choice routing, or other causal approximations to the expert-choice decision; evaluating these alternatives is an important future direction.

A second limitation is that the best-performing models in this work are hybrid models rather than pure MoSA models. Our results in Appendix C show that replacing all dense heads with MoSA heads generally underperforms, while retaining a small number of dense heads substantially improves performance. We hypothesize that the dense heads provide stable information flow while the MoSA heads learn specialized sparse routes; our long-sequence rolling-window results suggest that this role is not specific to dense attention.

The scale and context-length ranges studied here are also limited. We evaluate dense baselines up to 516M parameters and long sequences up to 8K tokens, which is sufficient to establish the method-level result that learned content-based sparse attention can outperform dense attention at matched FLOPs in this regime, but does not by itself establish behavior at frontier LLM scales or ultra-long contexts. The apparent reduction of relative gains at the largest model should also be interpreted carefully, because memory constraints limited the sparsity values we could evaluate at that scale (see Appendix D).

Finally, the downstream zero-shot results show that perplexity improvements do not always transfer uniformly to downstream tasks at the largest scale. Similar train-test and specialization effects have been observed in sparse and mixture-of-experts models (Nakamura et al., 2025; Shen et al., 2024b), and we report these results to make this behavior visible and encourage investigation.

Combining MoSA with other sparse attention patterns may be beneficial, since prior work often observes synergistic improvements from mixtures of sparse mechanisms on long sequences (Zaheer et al., 2020; Beltagy et al., 2020). Specialized CUDA kernels could further improve efficiency, and MoSA could be integrated with complementary approaches such as MQA (Shazeer, 2019), GQA (Ainslie et al., 2023), or SwitchHead (Csordás et al., 2024). Beyond autoregressive language modeling, MoSA may be useful in settings where non-autoregressive routing is natural, such as masked language modeling and vision transformers.

6 Conclusions

This paper introduces Mixture of Sparse Attention (MoSA), a novel attention architecture that selectively focuses on the most relevant tokens for each head, redirecting saved compute to create additional heads. MoSA reduces the computational complexity of attention from $O(T^2)$ to $O(k^2 + T)$, where T is the sequence length and k is the number of selected tokens per head. In our main experiments, MoSA is used in hybrid attention layers that retain four dense heads and replace the remaining dense heads with many MoSA heads.

Unlike other sparse attention methods that primarily show benefits for extremely long sequences, MoSA delivers substantial performance gains even in standard-length contexts. In this hybrid configuration, MoSA significantly outperforms both dense attention and sparse methods like fixed attention or the Routing Transformer, achieving up to 27% perplexity improvement over dense baselines across models of different scales, with dense baselines of up to 516M parameters. The comparison with fixed sparse attention suggests that these gains do not come merely from computing fewer projections or adding more heads, but from learned content-based selection. We also demonstrated that MoSA can be used to reduce the resource requirements of the models, including wall-clock time, memory usage, and the number of stored keys and values in a perplexity-matched setting. Because the current expert-choice router is non-autoregressive, these measurements should be interpreted as evidence of MoSA's potential for autoregressive models once a causal routing adaptation is developed, rather than as a completed deployment-ready inference method. Additionally, our results indicate that MoSA is promising in long-sequence scenarios, outperforming other sparse attention methods in these contexts as well.

The efficiency and corresponding performance gains demonstrated by MoSA have significant implications for the design of adaptive architectures. Overall, the results show that learned MoE-style sparsity in attention is a promising direction for building adaptive transformer architectures, and they identify causal routing, hybridization, scaling behavior, and downstream transfer as important directions for future work. While MoSA's gains are stable within the tested range of scales, whether they persist at frontier LLM scales remains an open question for future investigation.

References

Ashish Vaswani, Noam Shazeer, Niki Parmar, Jakob Uszkoreit, Llion Jones, Aidan N. Gomez, Lukasz Kaiser, and Illia Polosukhin. Attention is all you need. In *Proc. Advances in Neural Information Processing Systems (NIPS)*, pages 5998–6008, Long Beach, CA, USA, December 2017.

Tom Brown, Benjamin Mann, Nick Ryder, Melanie Subbiah, Jared D Kaplan, Prafulla Dhariwal, Arvind Neelakantan, Pranav Shyam, Girish Sastry, Amanda Askell, et al. Language models are few-shot learners. In *Proc. Advances in Neural Information Processing Systems (NeurIPS)*, pages 1877–1901, 2020.

Hugo Touvron, Thibaut Lavril, Gautier Izacard, Xavier Martinet, Marie-Anne Lachaux, Timothée Lacroix, Baptiste Rozière, Naman Goyal, Eric Hambro, Faisal Azhar, Aurélien Rodriguez, Armand Joulin, Edouard Grave, and Guillaume Lample. LLaMA: Open and efficient foundation language models. *Preprint arXiv:2302.13971*, 2023.

Gemini Team, Petko Georgiev, Ving Ian Lei, Ryan Burnell, Libin Bai, Anmol Gulati, Garrett Tanzer, Damien Vincent, Zhufeng Pan, Shibo Wang, et al. Gemini 1.5: Unlocking multimodal understanding across millions of tokens of context. *arXiv preprint arXiv:2403.05530*, 2024.

Aaron Grattafiori, Abhimanyu Dubey, Abhinav Jauhri, Abhinav Pandey, Abhishek Kadian, Ahmad Al-Dahle, Aiesha Letman, Akhil Mathur, Alan Schelten, Alex Vaughan, et al. The llama 3 herd of models. *arXiv preprint arXiv:2407.21783*, 2024.

Albert Gu, Tri Dao, Stefano Ermon, Atri Rudra, and Christopher Ré. Hippo: Recurrent memory with optimal polynomial projections. In *Proc. Advances in Neural Information Processing Systems (NeurIPS)*, volume 33, pages 1474–1487, 2020.

Albert Gu, Karan Goel, and Christopher Ré. Efficiently modeling long sequences with structured state spaces. In *Int. Conf. on Learning Representations (ICLR)*, 2022.

Albert Gu and Tri Dao. Mamba: Linear-time sequence modeling with selective state spaces. *arXiv preprint arXiv:2312.00752*, 2023.

Xiao Wang, Shiao Wang, Yuhe Ding, Yuehang Li, Wentao Wu, Yao Rong, Weizhe Kong, Ju Huang, Shihao Li, Haoxiang Yang, et al. State space model for new-generation network alternative to transformers: A survey. *arXiv preprint arXiv:2404.09516*, 2024.

Songlin Yang, Jan Kautz, and Ali Hatamizadeh. Gated delta networks: Improving mamba2 with delta rule. In *Int. Conf. on Learning Representations (ICLR)*, 2025.

Jongho Park, Jaeseung Park, Zheyang Xiong, Nayoung Lee, Jaewoong Cho, Samet Oymak, Kangwook Lee, and Dimitris Papailiopoulos. Can mamba learn how to learn? a comparative study on in-context learning tasks. In *Proc. Int. Conf. on Machine Learning (ICML)*, 2024.

Simiao Zuo, Xiaodong Liu, Jian Jiao, Denis Charles, Eren Manavoglu, Tuo Zhao, and Jianfeng Gao. Efficient long sequence modeling via state space augmented transformer. *arXiv preprint arXiv:2212.08136*, 2022.

Opher Lieber, Barak Lenz, Hofit Bata, Gal Cohen, Jhonathan Osin, Itay Dalmedigos, Erez Safahi, Shaked Meirom, Yonatan Belinkov, Shai Shalev-Shwartz, et al. Jamba: A hybrid transformer-mamba language model. *arXiv preprint arXiv:2403.19887*, 2024.

Angelos Katharopoulos, Apoorv Vyas, Nikolaos Pappas, and François Fleuret. Transformers are RNNs: Fast autoregressive transformers with linear attention. In *Proc. Int. Conf. on Machine Learning (ICML)*, volume 119, pages 5156–5165, Virtual Only, 2020.

Imanol Schlag, Kazuki Irie, and Jürgen Schmidhuber. Linear transformers are secretly fast weight programmers. In *Proc. Int. Conf. on Machine Learning (ICML)*, volume 139, pages 9355–9366, Virtual only, 2021.

Jürgen Schmidhuber. Learning to control fast-weight memories: An alternative to recurrent nets. *Neural Computation*, 4(1):131–139, 1992.

Zhen Qin, Xiaodong Han, Weixuan Sun, Dongxu Li, Lingpeng Kong, Nick Barnes, and Yiran Zhong. The devil in linear transformer. In *Proc. Conf. on Empirical Methods in Natural Language Processing (EMNLP)*, pages 7025–7041, 2022.

Rewon Child, Scott Gray, Alec Radford, and Ilya Sutskever. Generating long sequences with sparse transformers. *arXiv preprint arXiv:1904.10509*, 2019.

Manzil Zaheer, Guru Guruganesh, Kumar Avinava Dubey, Joshua Ainslie, Chris Alberti, Santiago Ontañon, Philip Pham, Anirudh Ravula, Qifan Wang, Li Yang, et al. Big bird: Transformers for longer sequences. In *Proc. Advances in Neural Information Processing Systems (NeurIPS)*, volume 33, pages 17283–17297, 2020.

Iz Beltagy, Matthew E. Peters, and Arman Cohan. Longformer: The long-document transformer. *arXiv:2004.05150*, 2020.

Simran Arora, Sabri Eyuboglu, Aman Timalsina, Isys Johnson, Michael Poli, James Zou, Atri Rudra, and Christopher Ré. Zoology: Measuring and improving recall in efficient language models. *Int. Conf. on Learning Representations (ICLR)*, 2024.

Samy Jelassi, David Brandfonbrener, Sham M Kakade, and Eran Malach. Repeat after me: Transformers are better than state space models at copying. In *Proc. Int. Conf. on Machine Learning (ICML)*, 2024.

Yi Tay, Dara Bahri, Donald Metzler, Da-Cheng Juan, Zhe Zhao, and Che Zheng. Synthesizer: Rethinking self-attention for transformer models. In *Proc. Int. Conf. on Machine Learning (ICML)*, pages 10183–10192, 2021.

Apoorv Vyas, Angelos Katharopoulos, and François Fleuret. Fast transformers with clustered attention. In *Proc. Advances in Neural Information Processing Systems (NeurIPS)*, volume 33, pages 21665–21674, 2020.

Aurko Roy, Mohammad Saffar, Ashish Vaswani, and David Grangier. Efficient content-based sparse attention with routing transformers. *Transactions of the Association for Computational Linguistics (TACL)*, 9:53–68, 2021.

Leon Bottou and Yoshua Bengio. Convergence properties of the k-means algorithms. In *Proc. Advances in Neural Information Processing Systems (NIPS)*, volume 7, 1994.

Noam Shazeer, Azalia Mirhoseini, Krzysztof Maziarz, Andy Davis, Quoc Le, Geoffrey Hinton, and Jeff Dean. Outrageously large neural networks: The sparsely-gated mixture-of-experts layer. In *Int. Conf. on Learning Representations (ICLR)*, Toulon, France, April 2017.

William Fedus, Barret Zoph, and Noam Shazeer. Switch transformers: Scaling to trillion parameter models with simple and efficient sparsity. *Journal of Machine Learning Research (JMLR)*, 23(1):5232–5270, 2022.

Yanqi Zhou, Tao Lei, Hanxiao Liu, Nan Du, Yanping Huang, Vincent Zhao, Andrew M Dai, Quoc V Le, James Laudon, et al. Mixture-of-experts with expert choice routing. In *Proc. Advances in Neural Information Processing Systems (NeurIPS)*, volume 35, pages 7103–7114, 2022.

Xiaofeng Zhang, Yikang Shen, Zeyu Huang, Jie Zhou, Wenge Rong, and Zhang Xiong. Mixture of attention heads: Selecting attention heads per token. In *Proc. Conf. on Empirical Methods in Natural Language Processing (EMNLP)*, pages 4150–4162, Abu Dhabi, United Arab Emirates, December 2022.

Róbert Csordás, Piotr Piękos, Kazuki Irie, and Jürgen Schmidhuber. Switchhead: Accelerating transformers with mixture-of-experts attention. In *Proc. Advances in Neural Information Processing Systems (NeurIPS)*, Vancouver, Canada, December 2024.

Zichang Liu, Aditya Desai, Fangshuo Liao, Weitao Wang, Victor Xie, Zhaozhuo Xu, Anastasios Kyrillidis, and Anshumali Shrivastava. Scissorhands: Exploiting the persistence of importance hypothesis for llm kv cache compression at test time. In *Proc. Advances in Neural Information Processing Systems (NeurIPS)*, volume 36, pages 52342–52364, 2023.

Yuhong Li, Yingbing Huang, Bowen Yang, Bharat Venkitesh, Acyr Locatelli, Hanchen Ye, Tianle Cai, Patrick Lewis, and Deming Chen. Snapkv: Llm knows what you are looking for before generation. In *Proc. Advances in Neural Information Processing Systems (NeurIPS)*, volume 37, pages 22947–22970, 2025.

Zefan Cai, Yichi Zhang, Bofei Gao, Yuliang Liu, Tianyu Liu, Keming Lu, Wayne Xiong, Yue Dong, Baobao Chang, Junjie Hu, and Xiao Wen. Pyramidkv: Dynamic kv cache compression based on pyramidal information funneling. *arXiv preprint arXiv:2406.02069*, 2024.

Dmitry Lepikhin, HyoukJoong Lee, Yuanzhong Xu, Dehao Chen, Orhan Firat, Yanping Huang, Maxim Krikun, Noam Shazeer, and Zhifeng Chen. Gshard: Scaling giant models with conditional computation and automatic sharding. In *Int. Conf. on Learning Representations (ICLR)*, 2021.

Noam Shazeer. Fast transformer decoding: One write-head is all you need. *arXiv preprint arXiv:1911.02150*, 2019.

Jingyang Yuan, Huazuo Gao, Damai Dai, Junyu Luo, Liang Zhao, Zhengyan Zhang, Zhenda Xie, YX Wei, Lean Wang, Zhiping Xiao, et al. Native sparse attention: Hardware-aligned and natively trainable sparse attention. *arXiv preprint arXiv:2502.11089*, 2025.

Róbert Csordás, Kazuki Irie, and Jürgen Schmidhuber. Approximating two-layer feedforward networks for efficient transformers. In *Findings of the Association for Computational Linguistics: EMNLP 2023*, November 2023.

Tri Dao, Daniel Y. Fu, Stefano Ermon, Atri Rudra, and Christopher Ré. FlashAttention: Fast and memory-efficient exact attention with IO-awareness. In *Proc. Advances in Neural Information Processing Systems (NeurIPS)*, New Orleans, Louisiana, USA, December 2022.

Adam Paszke, Sam Gross, Francisco Massa, Adam Lerer, James Bradbury, Gregory Chanan, Trevor Killeen, Zeming Lin, Natalia Gimelshein, Luca Antiga, Alban Desmaison, Andreas Kopf, Edward Yang, Zachary DeVito, Martin Raison, Alykhan Tejani, Sasank Chilamkurthy, Benoit Steiner, Lu Fang, Junjie Bai, and Soumith Chintala. PyTorch: An imperative style, high-performance deep learning library. In *Proc. Advances in Neural Information Processing Systems (NeurIPS)*, pages 8024–8035, Vancouver, Canada, December 2019.

Jianlin Su, Yu Lu, Shengfeng Pan, Bo Wen, and Yunfeng Liu. RoFormer: Enhanced transformer with rotary position embedding. *Preprint arXiv:2104.09864*, 2021.

Taku Kudo and John Richardson. Sentencepiece: A simple and language independent subword tokenizer and detokenizer for neural text processing. In *Proc. Conf. on Empirical Methods in Natural Language Processing (EMNLP)*, pages 66–71, Brussels, Belgium, October 2018.

Rico Sennrich, Barry Haddow, and Alexandra Birch. Neural machine translation of rare words with subword units. In *Proc. Association for Computational Linguistics (ACL)*, pages 1715–1725, Berlin, Germany, August 2016.

Mike Schuster and Kaisuke Nakajima. Japanese and korean voice search. In *Proc. IEEE Int. Conf. on Acoustics, Speech and Signal Processing (ICASSP)*, pages 5149–5152, Kyoto, Japan, March 2012.

Colin Raffel, Noam Shazeer, Adam Roberts, Katherine Lee, Sharan Narang, Michael Matena, Yanqi Zhou, Wei Li, and Peter J. Liu. Exploring the limits of transfer learning with a unified text-to-text transformer. *Journal of Machine Learning Research (JMLR)*, 21:140:1–140:67, 2020.

Diederik P. Kingma and Jimmy Ba. Adam: A method for stochastic optimization. In Yoshua Bengio and Yann LeCun, editors, *Int. Conf. on Learning Representations (ICLR)*, San Diego, CA, USA, May 2015.

Guangxuan Xiao, Yuandong Tian, Beidi Chen, Song Han, and Mike Lewis. Efficient streaming language models with attention sinks. In *Int. Conf. on Learning Representations (ICLR)*, 2024.

Nikita Kitaev, Kaiser Łukasz, and Anselm Levskaya. Reformer: The efficient transformer. In *Int. Conf. on Learning Representations (ICLR)*, 2020.

Chejian Xu, Wei Ping, Peng Xu, Zihan Liu, Boxin Wang, Mohammad Shoeybi, Bo Li, and Bryan Catanzaro. From 128k to 4m: Efficient training of ultra-long context large language models. *arXiv preprint arXiv:2504.06214*, 2025.

Krzysztof Marcin Choromanski, Valerii Likhosherstov, David Dohan, Xingyou Song, Andreea Gane, Tamás Sarlós, Peter Hawkins, Jared Quincy Davis, Afroz Mohiuddin, Lukasz Kaiser, David Benjamin Belanger, Lucy J. Colwell, and Adrian Weller. Rethinking attention with performers. In *Int. Conf. on Learning Representations (ICLR)*, Virtual only, May 2021.

Guoxuan Chen, Han Shi, Jiawei Li, Yihang Gao, Xiaozhe Ren, Yimeng Chen, Xin Jiang, Zhenguo Li, Weiyang Liu, and Chao Huang. Sepllm: Accelerate large language models by compressing one segment into one separator. *arXiv preprint arXiv:2412.12094*, 2024.

Aditya Desai, Shuo Yang, Alejandro Cuadron, Ana Klimovic, Matei Zaharia, Joseph E Gonzalez, and Ion Stoica. Hashattention: Semantic sparsity for faster inference. *arXiv preprint arXiv:2412.14468*, 2024.

Daya Guo, Dejian Yang, Haowei Zhang, Junxiao Song, Ruoyu Zhang, Runxin Xu, Qihao Zhu, Shirong Ma, Peiyi Wang, Xiao Bi, et al. Deepseek-r1: Incentivizing reasoning capability in llms via reinforcement learning. *arXiv preprint arXiv:2501.12948*, 2025.

Albert Q Jiang, Alexandre Sablayrolles, Antoine Roux, Arthur Mensch, Blanche Savary, Chris Bamford, Devendra Singh Chaplot, Diego de las Casas, Emma Bou Hanna, Florian Bressand, et al. Mixtral of experts. *arXiv preprint arXiv:2401.04088*, 2024.

Yikang Shen, Zhen Guo, Tianle Cai, and Zengyi Qin. Jetmoe: Reaching llama2 performance with 0.1 m dollars. *arXiv preprint arXiv:2404.07413*, 2024a.

Mike Lewis, Shruti Bhosale, Tim Dettmers, Naman Goyal, and Luke Zettlemoyer. BASE layers: Simplifying training of large, sparse models. In Marina Meila and Tong Zhang, editors, *Proc. Int. Conf. on Machine Learning (ICML)*, volume 139, pages 6265–6274, Virtual only, July 2021.

Stephen Roller, Sainbayar Sukhbaatar, Jason Weston, et al. Hash layers for large sparse models. In *Proc. Advances in Neural Information Processing Systems (NeurIPS)*, volume 34, pages 17555–17566, 2021.

David Raposo, Sam Ritter, Blake Richards, Timothy Lillicrap, Peter Conway Humphreys, and Adam Santoro. Mixture-of-depths: Dynamically allocating compute in transformer-based language models. *arXiv preprint arXiv:2404.02258*, 2024.

Peng Jin, Bo Zhu, Li Yuan, and Shuicheng Yan. Moh: Multi-head attention as mixture-of-head attention. *arXiv preprint arXiv:2410.11842*, 2024.

Taishi Nakamura, Satoki Ishikawa, Masaki Kawamura, Takumi Okamoto, Daisuke Nohara, Jun Suzuki, and Rio Yokota. Optimal sparsity of mixture-of-experts language models for reasoning tasks. *arXiv preprint arXiv:2508.18672*, 2025.

Sheng Shen, Le Hou, Yanqi Zhou, Nan Du, Shayne Longpre, Jason Wei, Hyung Won Chung, Barret Zoph, William Fedus, Xinyun Chen, et al. Mixture-of-experts meets instruction tuning: A winning combination for large language models. In *Int. Conf. on Learning Representations (ICLR)*, 2024b.

Joshua Ainslie, James Lee-Thorp, Michiel de Jong, Yury Zemlyanskiy, Federico Lebrón, and Sumit Sanghai. Gqa: Training generalized multi-query transformer models from multi-head checkpoints. In *Proc. Conf. on Empirical Methods in Natural Language Processing (EMNLP)*, pages 4895–4901, 2023.

Qingru Zhang, Dhananjay Ram, Cole Hawkins, Sheng Zha, and Tuo Zhao. Efficient long-range transformers: You need to attend more, but not necessarily at every layer. In *Proc. Conf. on Empirical Methods in Natural Language Processing (EMNLP)*, 2023.

Ruibin Xiong, Yunchang Yang, Di He, Kai Zheng, Shuxin Zheng, Chen Xing, Huishuai Zhang, Yanyan Lan, Liwei Wang, and Tie-Yan Liu. On layer normalization in the transformer architecture. In *Proc. Int. Conf. on Machine Learning (ICML)*, volume 119, pages 10524–10533, Virtual Only, July 2020.

Barret Zoph, Irwan Bello, Sameer Kumar, Nan Du, Yanping Huang, Jeff Dean, Noam Shazeer, and William Fedus. St-moe: Designing stable and transferable sparse expert models. *arXiv preprint arXiv:2202.08906*, 2022.

Denis Paperno, Germán Kruszewski, Angeliki Lazaridou, Quan Ngoc Pham, Raffaella Bernardi, Sandro Pezzelle, Marco Baroni, Gemma Boleda, and Raquel Fernández. The LAMBADA dataset: Word prediction requiring a broad discourse context. In *Proc. Association for Computational Linguistics (ACL)*, Berlin, Germany, August 2016.

Keisuke Sakaguchi, Ronan Le Bras, Chandra Bhagavatula, and Yejin Choi. Winogrande: An adversarial winograd schema challenge at scale. In *Proc. AAAI Conf. on Artificial Intelligence*, pages 8732–8740, New York, NY, USA, February 2020.

Alex Warstadt, Alicia Parrish, Haokun Liu, Anhad Mohananey, Wei Peng, Sheng-Fu Wang, and Samuel R. Bowman. BLiMP: The benchmark of linguistic minimal pairs for English. *Transactions of the Association for Computational Linguistics (TACL)*, 8:377–392, 2020.

Rowan Zellers, Ari Holtzman, Yonatan Bisk, Ali Farhadi, and Yejin Choi. Hellaswag: Can a machine really finish your sentence? In *Proc. Association for Computational Linguistics (ACL)*, pages 4791–4800, Florence, Italy, August 2019.

Yonatan Bisk, Rowan Zellers, Ronan Le Bras, Jianfeng Gao, and Yejin Choi. PIQA: reasoning about physical commonsense in natural language. In *Proc. AAAI Conf. on Artificial Intelligence*, pages 7432–7439, New York, NY, USA, February 2020. AAAI Press.

Peter Clark, Isaac Cowhey, Oren Etzioni, Tushar Khot, Ashish Sabharwal, Carissa Schoenick, and Oyvind Tafjord. Think you have solved question answering? try ARC, the AI2 reasoning challenge. *Preprint arXiv:1803.05457*, 2018.

A Baselines

Apart from a dense baseline, we compare MoSA with two sparse attention methods: static, position-based sparse attention, and content-based sparse attention.

We visualize typical schematic attention patterns of the baselines and MoSA in Fig. 2. Note that several previous works proposed combining different types of sparse attention to achieve synergic performance in long-sequence tasks (Beltagy et al., 2020; Zaheer et al., 2020; Zhang et al., 2023). In this work, we focus on investigating sparse attention methods in combination with a few dense attention heads, but without combining multiple sparse attention types. We leave combining MoSA with other sparse-attention methods for future work.

Fixed Sparse Attention. Position-based static attention patterns have been shown to be a strong sparse attention variant (Child et al., 2019), outperforming strided sliding window attention. Fixed sparse attention for a sparsity ρ selects $k = \frac{T}{\rho}$ tokens with stride ρ. Using the notation introduced in Section 2.2, fixed sparse attention can be written as a special case of MoSA, where $I = [0, \rho, 2\rho, ..., T - \rho]$ and $\mathbf{r} = \mathbf{1}$.

Fixed sparse attention reduces computational complexity in two ways. First, it decreases the $O(T^2)$ cost of the full attention matrix by limiting attention to predefined token positions. Second, since only these pre-selected tokens participate in attention calculations, the query, key, value, and output transformations need only be computed for this subset rather than all tokens. This is important because MoSA also benefits from calculating transformations only for a selected subset of tokens. Hence, investigating this fixed sparse attention gives insight on whether pure benefits of sparsifying over transformations can lead to performance improvements.

However, fixed sparse attention introduces information flow constraints. Pre-selected tokens must aggregate necessary information in earlier layers. Furthermore, in the subsequent layers they have to be routed back to the positions where they are most useful. This additional overhead in information routing limits the model's representational capacity and overall expressiveness.

The Routing Transformer. We also compare MoSA to the content-based attention proposed in the Routing Transformer (Roy et al., 2021). The Routing Attention is the most similar method to MoSA we found in the literature. It groups tokens with online K-means into ρ clusters of size $k = \frac{T}{\rho}$ *inside* each head. This is implemented during training by the top-k tokens most similar to the cluster centers using the dot-product distance metric. Cluster centers are learned using a moving average of the most similar tokens.

The Routing Attention might resemble the Expert-Choice selection with MoSA. There are, however, several crucial differences that, as our experiments show, lead to significant differences in the performance of MoSA in comparison to the Routing Transformer. Specifically, online K-means, used for clustering in the Routing Transformer is known for suffering from an extremely slow convergence rate (Bottou and Bengio, 1994). It is also unclear if clustering keys and queries is well aligned with the language modeling objective. In contrast, the learned dynamic matching mechanism of MoSA is directly optimized by the same objective as the model.

MoSA benefits from the sparsity in the $\mathbf{W}^Q, \mathbf{W}^K, \mathbf{W}^V, \mathbf{W}^O$ transformations, which need to be computed only for selected tokens. In contrast, the Routing Transformer has to compute all keys and queries before the clustering step. MoSA's efficiency enables the use of more heads with specialized weights in a smaller subset of tokens. Its selection can also lead to dynamic compute allocation, where some more important tokens are processed by more heads than less important tokens.

Last but not least, the Routing Transformer performs best in language modeling when the clusters share the same destination (query) tokens and source (keys and values) tokens. In our experiments, we also found that MoSA performs better if the same tokens are selected for the source and destination sides. However, to enforce this in the Routing Transformer, they require to set $\mathbf{W}^Q = \mathbf{W}^K$. In MoSA, however, the same selection for source and destination side can be enforced with $\mathbf{W}^Q$ different from $\mathbf{W}^K$, allowing greater flexibility.

We visualize typical schematic attention patterns of the baselines and MoSA in Fig. 2. Note that several previous works proposed combining different types of sparse attention to achieve synergic performance in long-sequence tasks (Beltagy et al., 2020; Zaheer et al., 2020; Zhang et al., 2023). In this work, we focus on investigating sparse attention methods in combination with a few dense attention heads, but without combining multiple sparse attention types. We leave combining MoSA with other sparse-attention methods for future work.

Mixture of Attention Heads Mixture of Attention Heads (MoA) (Zhang et al., 2022) addresses the instability of applying Mixture-of-Experts (MoE) to attention mechanisms by enforcing shared key and value projections across all heads, following the MQA design (Vyas et al., 2020). Expert sparsity is applied only to the query transformation. Because all heads use the same key and value mappings, discrepancies between expert-routed queries and the fixed keys/values are avoided: the shared projections are trained to be universally compatible with all query experts. This stabilizes training and enables scaling to many heads. However, MoA inherits a core limitation of MQA: since key and value projections are fixed regardless of head count, scaling the number of heads yields diminishing returns, as only the query pathway benefits from expert specialization.

Native Sparse Attention Native Sparse Attention (NSA) (Yuan et al., 2025) proposes to calculate fine-grained attention only for selected blocks based on proximity scores calculated from aggregated information across tokens from a given block. This reduces the necessity of calculating the entire matrix of attention, and therefore leads to significant efficiency improvements in comparison to the dense baseline. NSA, however, does not sparsify QK transformations, and therefore is not suitable for the design proposed by us in this paper with a lot of small attention heads.

B FLOPs cost derivation

In this section, we derive the FLOP cost for dense and MoSA heads, and the total FLOPs necessary for the forward pass of each model.

Multiplying matrices of shape $[i, j]$ and $[j, k]$ takes precisely $(2j - 1)ik$ FLOPs. For simplicity, following common practice, we approximate it by $2jik$.

In the dense attention layer, calculating each projection (e.g., $Q_i = xW_{Q_i}$) requires $2hh'T$ FLOPs. Computing the attention matrix $QK^\top$, and multiplying the attention matrix by values V both cost $2h'T^2$ FLOPs.

Calculating the projections and attention in the MoSA head is identical, except that now we are operating on k tokens instead of T. The MoSA head involves an additional routing overhead. Calculating the routing scores costs $2hT$ FLOPs, and multiplying the intermediate values in the matrix $\in \mathbb{R}^{k \times h'}$ by the scores costs an additional $h'k$ FLOPs per head.

The cost of a single head of the dense and MoSA heads are:

$$\text{FLOP}_{\text{dense}} = \underbrace{8hh'T}_{\text{Q,K,V,O mappings}} + \underbrace{4h'T^2}_{\text{Attention}}$$

$$\text{FLOP}_{\text{mosa}} = \underbrace{8hh'k}_{\text{Q,K,V,O mappings}} + \underbrace{4h'k^2}_{\text{Attention}} + \underbrace{2hT + h'k}_{\text{routing overhead}}$$

$$\text{FLOP}_{\text{fixed}} = \underbrace{8hh'k}_{\text{Q,K,V,O mappings}} + \underbrace{4h'k^2}_{\text{Attention}}$$

$$\text{FLOP}_{\text{routing}} = \underbrace{6hh'T}_{\text{Q=K,V,O mappings}} + \underbrace{4h'k^2\rho}_{\text{Attention}} + \underbrace{2h'T}_{\text{cluster selection}} = \rho(6hh'k + 4h'k^2) + 2h'T$$

For the multihead version, the FLOPs are multiplied by the number of heads H. There is an additional cost caused by summing the head contributions to a single output (Equations 2 and 3). However, this is already taken into account by the $2hh'TH$ cost of the output projection for multiple heads: $H(2h'-1)hT+(H-1)hT = (2h'H - 1)hT \approx 2hh'TH$.

Note that in the standard notation (Vaswani et al., 2017), the heads are first concatenated and then transformed with a single output projection instead of splitting the output operation into individual head transformations and summing. However, the result and the derivation of the FLOP counts are the same.

In the feedforward block, the intermediate layer has a typical size of $4h$. Therefore, the cost of the block is equal to $16h^2T$. Therefore, the FLOP cost of the forward pass of the entire model with l layers, a hybrid attention with H_{dense} dense heads and H_{mosa} MoSA heads is equal to:

$$lH_{dense}(8hh'T + 4h'T^2) + lH_{mosa}(8hh'k + 4h'k^2 + 2hT + h'k) + 16lh^2T$$

We omit the operations related to layer normalizations, residuals, and token embeddings from the FLOP calculations as they are negligible compared to the rest and represent an identical overhead for both dense and MoSA models. Thus, incorporating them does not influence the FLOP-matching process. This is also true for the feedforward block; yet, we still included it because it constitutes a significant portion of the total cost. We present the FLOP cost of all of our model classes (*Tiny, Small, Medium* and *Large*) in Table 6.

All models are based on the transformer architecture with Pre-layer normalisation(Xiong et al., 2020). Each model class *Tiny, Small, Medium* and *Large* follows the hyperparameters of the dense model. The necessary forward pass FLOPs are calculated according to App. B. The number of heads in the sparse models is set so that the resulting model is FLOP-matched to the dense baseline as closely as possible. When this is not perfectly possible, we ensure that its FLOP count never exceeds that of the baseline. For pure MoSA, all heads are replaced with MoSA heads. For the hybrid sparse models, 4 dense heads are kept, and the remaining ones are replaced with sparse heads.

C Analysing Hybrid Models

While the learned sparse attention can theoretically capture any attention pattern, the introduction of the routing mechanism complicates the learning dynamics. The router and the attention weights must be

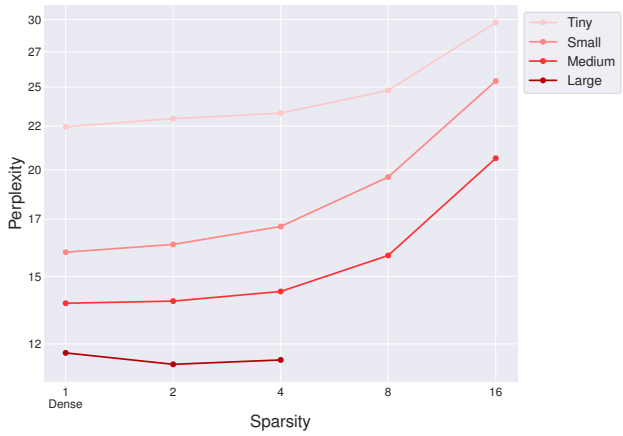

Figure 5: Perplexity of IsoFLOP matching models under pure MoSA setting. Each curve corresponds to a given FLOP budget. For a given sparsity, we replace all dense heads with a FLOP equivalent number of MoSA heads. In contrast to Fig 3, sparse models fail to outperform the baseline (apart from the Large model). This demonstrates the symbiotic relation between dense heads and MoSA heads in the hybrid model.

learned jointly. The router needs to identify relevant token pairs, while the attention weights learn to process these selected interactions. This interdependence can lead to training instabilities, particularly in the early stages, when router decisions are largely random. Poor initial routing can prevent attention heads from learning meaningful patterns, while the lack of meaningful patterns prevents the router from learning to select important tokens, creating a vicious circle.

Our preliminary experiments have shown that pure MoSA models without additional dense heads fail to improve the perplexity of dense baselines. To verify this, we conducted a study similar to our main results in Sec. 3.1. We gradually increase the sparsity by replacing all dense heads with MoSA heads while maintaining an identical FLOP count to the baseline. We do this by finding the maximum number of MoSA heads for which the FLOP count remains lower than the baseline. The results, shown in Fig. 5, demonstrate that increasing sparsity monotonically worsens model performance in most settings. This performance degradation with pure MoSA heads likely stems from the stability issues explained in the previous paragraph.

Interestingly, the largest model is an exception, and initially there is a visible improvement from 12.20 baseline perplexity to 11.83 perplexity of the FLOP-matched pure MoSA model with sparsity 2. This is still significantly worse than the 10.58 perplexity of the hybrid model with sparsity 4. Moreover, the saturation is much faster than for hybrid models. For hybrid models, the sparsity around 32 or 64 seems to be optimal. In contrast, for the MoSA-only model, the best perplexity is reached for sparsity 2 for the *Large* budget and 1 for the smaller ones. However, the conclusion is consistent across all scales: hybrid MoSA models significantly outperform MoSA-only models, which generally underperform the dense baseline. Thus, hybridization seems necessary.

The impact of sparsification is also visible in the training characteristics. Compared to the baseline, pure MoSA models start to plateau faster. While the losses of dense and hybrid models continue to show steep initial improvement, pure MoSA models slow down much sooner. This supports our hypothesis about the difficulty of learning the routing and attention simultaneously. We compare the training losses in Fig. 6.

Optimal Number of Dense Heads Hybrid models consistently outperform pure MoSA models. This raises a natural question: What is the optimal ratio of dense to sparse heads and how does this ratio relate to the sparsity rate?

To answer these questions, we conducted a series of experiments in which we varied both the sparsity factor of MoSA heads and the number of dense heads while keeping the total FLOP budget constant. We choose to use the *small* model and investigate sparsities $\rho = 4$ and $\rho = 16$, while we set the number of dense heads in the hybrid model from 0 to 9 (full dense model) and adapt the number of sparse heads to match the FLOP

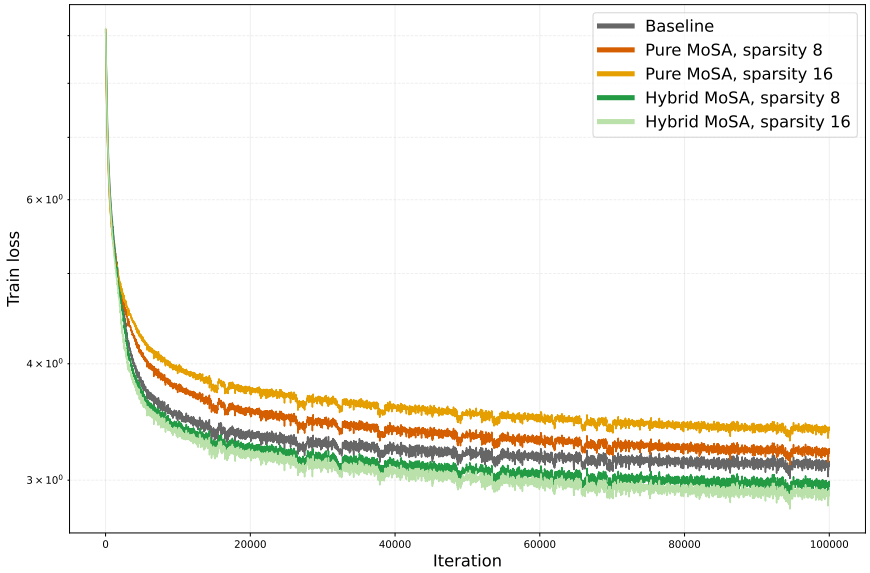

Figure 6: Training losses of the Tiny models comparing the baseline, pure MoSA, and hybrid models. The dense baseline clearly divides the models into two groups: all pure MoSA models perform worse (higher loss), while all hybrid models demonstrate superior performance (lower loss). Notably, increasing sparsity intensifies the difference for both model types: hybrid models achieve progressively lower loss with greater sparsity, whereas pure MoSA models show increasingly higher loss as sparsity increases. Additionally, the early training phase (between 5,000 and 10,000 steps) reveals a distinct pattern where pure MoSA models experience a more rapid slowdown in their learning progress compared to both dense and hybrid models.

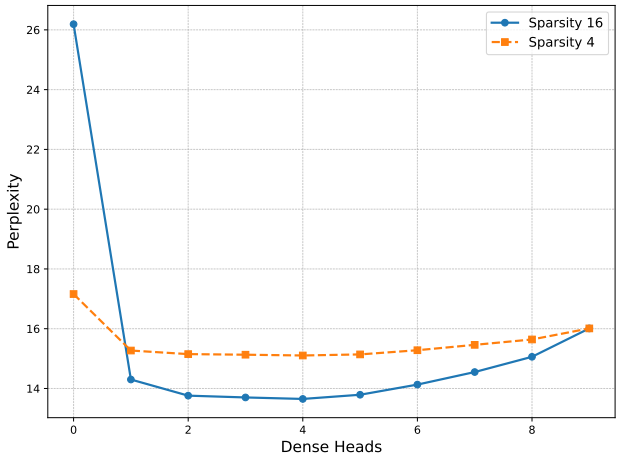

Figure 7: Perplexity of the FLOP matched models with a different number of dense heads for sparsities 4 and 16. 9 dense heads correspond to the dense baseline.

budget. Our results are shown in Fig. 7. We can see that the optimal number of dense heads in this case is 4 and is sparsity-agnostic. Because of this, we chose to use 4 dense heads in our main experiments in Sect. 3.1. Furthermore, we observe that it is critical to have at least one dense head. Having more than one has diminishing returns, and having more than 4 has a negative effect on the performance. The plot also shows that the lack of dense heads is more hurtful for models with higher sparsities. We conclude that in our case, 4 heads are sufficient to stabilize the training, and it is better to allocate the remaining FLOP budget to the more efficient MoSA heads.

D Scale and the Large-Model Trend

In Table 1, the relative improvement of MoSA over the dense baseline appears to shrink with scale, from 27.0% for *Tiny* to 13.3% for *Large*. This apparent diminishing trend comes from comparing the best observed sparsity at each scale, even though we could not evaluate the same sparsity range for all scales: at the largest scale, memory constraints prevented us from evaluating the higher sparsity range that was optimal for smaller models (see Section 3.1). When we compare the same sparsity values across scales, there is no clear diminishing pattern, as shown in Table 3.

	Dense	MoSA $\rho = 2$		MoSA $\rho = 4$	
Scale	ppl ↓	ppl ↓	Gain	ppl ↓	Gain
Tiny	22.46	21.76	−3.12%	20.45	−8.95%
Small	16.01	15.74	−1.69%	15.10	−5.68%
Medium	13.95	13.52	−3.08%	12.81	−8.17%
Large	12.20	11.33	−7.13%	10.58	−13.28%

Table 3: Perplexity of hybrid MoSA at fixed sparsities $\rho = 2$ and $\rho = 4$ across all model scales, compared to the dense baseline. Gain is the relative perplexity reduction. At the same sparsity, the gains do not diminish with scale; the largest model in fact shows the largest gain at both sparsities.

Thus, the 13.3% improvement at the *Large* scale should be read as the best result under the sparsities we could evaluate at that scale, not as evidence that the optimal MoSA gain shrinks monotonically with scale. A scaling-law analysis would be very valuable, but a clean study has several interacting variables to control: sparsity, the number of dense heads, the total number of sparse heads, depth, width, and training budget. We consider scaling-law-style analysis and larger-scale experiments important future work.

E Sparsity Patterns

MoSA's central mechanism is the learned, head-specific selection of tokens. The IsoFLOP experiments show that this mechanism improves perplexity compared to dense attention and to the tested sparse baselines, but they do not by themselves explain what the routers learn. In this appendix, we therefore analyze the selected token sets to test whether MoSA heads collapse to similar selections or instead learn diverse sparsity patterns across heads. For the experiments in this section we used Hybrid MoSA model with medium size and sparsity 4 in order to make the heads easier to manually interpret. All quantitative results in this appendix are computed on four hand-written example sentences and serve as an illustrative case study of the learned selection behavior, not as an estimate of a distribution over a held-out corpus.

E.1 Selection Diversity Across Heads

We first quantify diversity across heads. For each layer, we compare the selected token sets of pairs of MoSA heads using overlap measures such as the Jaccard index, $J(A, B) = |A \cap B|/|A \cup B|$. Low average overlap indicates that different heads are not selecting the same high-scoring tokens, while layer-wise trends show whether diversity changes across depth. These statistics complement the fixed sparse attention baseline: fixed sparse attention uses the same deterministic selection pattern across heads and performs worse than dense attention, whereas MoSA can allocate different heads to different content-dependent token subsets.

We measured pairwise Jaccard overlap between all sparse-head pairs in the hybrid MoSA model at sparsity 4 on the four hand-written sentences. The average overlap is moderate across the network: heads share some salient tokens, but they are far from selecting identical subsets. The mean pairwise Jaccard is 0.38 across all layers, far from the value of 1.0 that would indicate identical selections. We additionally observe a depth pattern (Table 4, Figure 8): the first layer is highly redundant, with many heads attending to the same determiners and clause separators (mean $J = 0.71$), while the late layers diversify, with the mean dropping to $J \approx 0.24$. Futhermore, we observe a pattern, that the heads at first layers very frequently select separators and non-informative tokens such as determiners. This pattern has been before utilized by researchers who

manually propose sparse attention patterns based on separators (Chen et al., 2024). Apart from early layers behave as syntactic anchors, we observe that late layers diverse more and have head-specific content. We analyze specific heads in Section E.2.

Layer group	Mean J	Std.	10th pct.	90th pct.
Early layers (0–5)	0.43	0.24	0.17	0.71
Middle layers (6–11)	0.45	0.20	0.20	0.67
Late layers (12–17)	0.27	0.18	0.09	0.50
All layers	0.38	0.22	0.12	0.65

Table 4: Pairwise Jaccard overlap between selected token sets of MoSA heads, computed over the four hand-written example sentences and all $\binom{26}{2}$ head pairs in each layer. The statistics illustrate the trend on these examples rather than a corpus-level distribution. Overlap is moderate overall; it is highest in the first layer and lowest in the late layers, indicating that diversification of head selections happens predominantly in the deeper part of the network.

Figure 8 shows the per-layer mean: In the first layer there is a significant redundancy of selection ($J = 0.71$). We also manually observe that this selection usually focuses on separators and determiners. the middle range hovers around 0.30–0.53, and the last six layers fall to a low plateau ($J \approx 0.23$–0.36) demonstrating high diversity. This, together with the results that compare to fixed sparse attention demonstrate that additional sparse heads are not redundant copies of one another, especially in the late layers: the router often agrees on attention-sink positions, but distributes the remaining token budget across different content-dependent views of the sequence. However, the plots in this section suggest possible improvements to experiment with, such as having more heads in later layers.

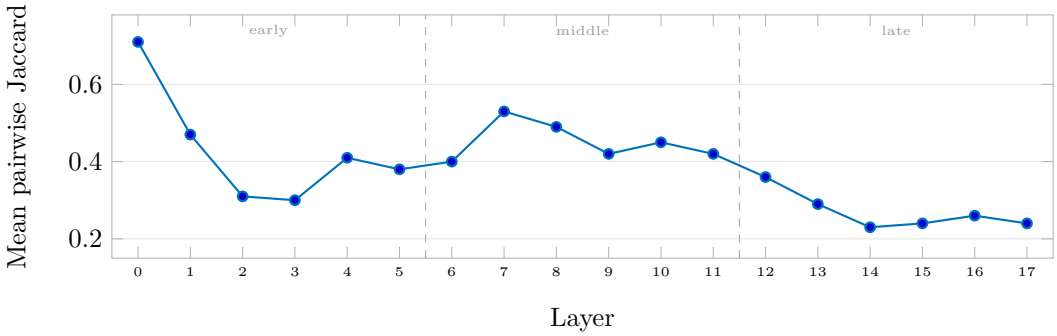

Figure 8: Per-layer mean pairwise Jaccard overlap between tokens selected by MoSA heads, computed on the four hand-written example sentences (illustrative).

E.2 Qualitative Head Examples

We also inspect individual examples to make the statistical diversity easier to interpret. Rather than visualizing a single sentence or a single layer, we compare manually selected heads from different depths across four sentences, which makes recurring head-specific tendencies and the depth-wise change in selection style easier to see. The goal is not to claim a complete taxonomy of heads, but to show concrete examples ranging from early-layer determiner anchors to late-layer content routers. Together with the aggregate overlap statistics, these examples provide a mechanistic view of how MoSA uses its many sparse heads.

Figure 9 shows the selections of seven MoSA heads spanning five different depths (layers 0, 2, 8, 14, and 17). One head is drawn from each of layers 0, 2, 8, and 14 to illustrate the depth-wise change in routing style; the remaining three heads are taken from the last layer (layer 17) to illustrate the diversity of head specialization *within* a single layer. Two recurring patterns are immediately visible. First, early layers concentrate on semantically thin tokens: the layer-0 head repeatedly fires on *the* and on commas, contributing

little content-level information but explaining the high $J = 0.71$ overlap of layer 0 heads. Second, the first token (BOS) is selected by several mid- and late-layer heads but *not* by the early-layer or pure-content heads, suggesting that attention-sink behavior emerges with depth rather than being uniform across the network. Within the last layer, the displayed heads spread their selections across content phrases, determiner/modifier clusters, and function words, indicating that single-layer head diversity is substantial even after accounting for the BOS sink.

These examples are consistent with the aggregate overlap results: heads are not merely selecting a common set of globally important tokens, but instead specialize in different views of the same sequence, with the specialization most pronounced in the late layers. Two recurring structural patterns deserve particular emphasis. First, the early layers contain heads that fire almost exclusively on syntactically thin tokens: determiners and clause separators, which explains the high overlap in the first layer ($J = 0.71$). Second, BOS is selected by most mid- and late-layer heads but *not* by the layer-0 or pure-content heads, which resembles the "attention sink" behavior observed in dense transformers: deeper heads reserve part of their sparse budget for a stable sequence-level anchor while spending the rest on head-specific content. Although the labels in Fig. 9 are informal, the seven highlighted heads can be loosely named after the token types they tend to select.

- **L0/H11, determiners and commas (early-layer):** this head repeatedly selects the determiner *the* (typically four times per sentence) together with commas, with very little content-word selection. It is representative of the densely-overlapping early-layer heads that drive the layer-0 Jaccard up to 0.71.
- **L2/H23, pure content selector:** this head selects only content tokens: *recipe, sugar, butter, cream, delivery, door, rain, library, notebook, page, topic, yesterday, night* with no determiners, no punctuation and no BOS or period sink.
- **L8/H12, BOS + determiner-plus-preposition cluster (mid-layer):** this head fixes the BOS anchor in every sentence and otherwise selects determiners and short prepositions and connectives such as *for*, *near*, *in*, *before*, and *during*, suggesting tracking of nominal and prepositional phrase boundaries.
- **L14/H21, late content with final-period anchor:** this head consistently selects the final period and the cluster of content tokens near the end of the sentence (*cream/today*, *door/night/rain*, *topic/yesterday/night*, *blank*), without using BOS as an anchor. It illustrates how the late-layer routing diverges from the BOS-sink pattern.
- **L17/H9, content phrases:** this head tends to select content-heavy phrases while avoiding many pure function tokens, for example ingredient tokens (*sugar*, *butter*, *cream*) in the recipe sentence and the *final/page* cluster in the notebook sentence. Notably, BOS is not always selected by this head, indicating that not all last-layer heads share the attention-sink anchor.
- **L17/H14, determiners and modifiers:** this head often selects determiners together with nearby adjective or modifier tokens, including repeated *the* tokens and words such as *old*, *difficult*, *missing*, and *final*.
- **L17/H22, function words:** this head is biased toward function words and relational tokens, including determiners and prepositions such as *the*, *for*, *before*, *near*, *during*, and *in*, which complements the content-routing behavior of L17/H0 and L17/H9 within the same layer.

The selections do not perfectly correspond to these rough names, and the degree of specialization varies along two axes. Across depth: early layers are dominated by determiner repetition, layer 2 contains a small set of pure content specialists, mid-layers mix attention sinks with structural cues, and the late layers route to head-specific content with the lowest pairwise overlap of the network. Within the last layer: heads spread their selections across content phrases, determiner/modifier clusters, and function words, indicating that head diversity is substantial *within* a single layer and not only across depth. This combined depth- and within-layer

organization: Thin syntactic anchoring early, diverse content and structural routing late, mirrors the per-layer Jaccard curve in Figure 8 and suggests that sparse routing in MoSA is not random: after accounting for the BOS and determiner anchors, different heads allocate their remaining budget to different structural or semantic aspects of the sentence. A more systematic inspection of attention patterns and MoSA selection patterns is therefore a promising direction for future work.

F Downstream Tasks

Additionally we evaluate the tuned results on downstream tasks to inspect the performance of the sparse models. Note, that usually sparse models suffer performance drops on downstream tasks and additional fine-tuning has been shown to mitigate this. First, MoE architectures have been shown to suffer from expert overspecialization, which often leads to decreased performance in downstream tasks (Fedus et al., 2022; Zoph et al., 2022). Instruction tuning has been shown to mitigate this issue (Shen et al., 2024b). Furthermore, content-based sparse attention methods tend to struggle on shorter sequence[‡]. Nevertheless we provide the investigation of downstream results for a comprehensive evaluation.

We evaluate the zero-shot downstream performance of MoSA on six established benchmarks: LAMBADA (Paperno et al., 2016), WinoGrande (Sakaguchi et al., 2020), BLiMP (Warstadt et al., 2020), HellaSwag (Zellers et al., 2019), PIQA (Bisk et al., 2020) and AI2ARC (Clark et al., 2018)—covering tasks from cloze-style completion to commonsense reasoning.

During training, MoSA operates on sequences of more or less constant size $T = 1024$. However, for downstream tasks, some inputs will be much shorter. For example, most datapoints in the BLiMP dataset do not exceed 10 tokens. In order to handle such situations, we adaptively choose the number of tokens for each input to be $k = \max(\lfloor \frac{T}{\rho} \rfloor, 2)$ tokens for each head. This simulates the ratio of tokens selected for the attention head during the training. Moreover, it ensures that at least 2 tokens are selected, which is the minimum necessary for the attention to model any cross-token dependencies.

For each scale and sparse model type, we select the model with sparsity $\rho > 1$ that produced the best perplexity in the IsoFLOP scenario (Sec. 3.1). We also include the dense baseline for each size. Table 5 reports the performance across the tasks. The best result for a given task across model types is bold.

For *Tiny*, *Small*, and *Medium* scales, MoSA generally outperforms other models. BLiMP stands as a notable exception, where MoSA consistently underperforms. This weak performance on BLiMP can be attributed to the extremely short length of most examples in the dataset. With longer sequences seen during training, each MoSA head can selectively process only the tokens it handles well. However, in short sequences, the shortage of tokens forces MoSA heads to operate on tokens outside their training distribution. Furthermore, when $\lfloor \frac{T}{\rho} \rfloor = 1$, resulting in only 2 tokens being selected, there is a significant discrepancy between the percentage of selected tokens compared to training conditions. Models with a high sparsity factor of 64 typically select only 1.56% tokens in a sequence for each attention head. Yet for a sequence length of $T = 10$, 2 selected tokens represent 20% of the sentence, creating a distribution mismatch.

G Details of the Models

In Table 6 we list hyperparameters of all dense baselines.

[‡]See: `https://github.com/lucidrains/routing-transformer?tab=readme-ov-file#issues`

	Model	LAMBADA	WinoGrande	BLiMP	HellaSwag	PIQA	AI2ARC
Tiny	Dense	18.7	50.3	72.0	27.5	**59.4**	28.0
	MoSA	**25.4**	**51.9**	64.6	**29.1**	**59.4**	**28.6**
	Routing	14.0	51.3	66.2	27.8	57.1	25.9
	Fixed	17.1	50.6	**72.5**	27.7	58.6	28.1
Small	Dense	25.8	**52.1**	**76.2**	30.9	62.4	30.1
	MoSA	**30.7**	48.5	62.8	**31.8**	60.4	**30.2**
	Routing	19.2	50.7	70.2	28.0	57.6	27.3
	Fixed	24.6	51.6	75.3	30.1	**63.2**	**30.2**
Medium	Dense	**31.4**	51.2	**77.8**	33.8	64.5	31.5
	MoSA	27.6	**52.2**	75.1	**33.9**	**65.1**	**31.6**
	Routing	10.2	51.5	65.9	30.3	57.8	27.8
	Fixed	29.4	51.4	77.3	33.0	64.6	31.5
Large	Dense	**36.2**	52.5	**80.4**	**38.7**	**67.1**	**33.8**
	MoSA	32.3	**52.8**	77.2	36.6	65.0	32.2
	Routing	27.5	51.1	76.5	36.2	64.1	32.5
	Fixed	32.3	51.7	79.6	35.9	66.0	32.2

Table 5: Accuracy on downstream zero-shot tasks. Each model is selected with the best sparsity in the IsoFLOP comparison. Note that on downstream tasks, the token selection mechanism of MoSA operates out of distribution. Despite this, MoSA often outperforms the dense baseline. Even when it doesn't, the performance gap is usually small.

	Tiny	**Small**	**Medium**	**Large**
FLOPs per pass (G)	54.76	219.85	430.70	1,130.65
Layers	6	9	18	27
Hidden size	512	1,024	1,024	1,280
Feedforward hidden size	2,048	4,096	4,096	5,120
Head hidden size	64	64	64	64
Number of heads	9	9	9	16

Table 6: Hyperparameters of the different model variants and the corresponding FLOP cost of the forward pass for a sequence length of $T = 1024$.

		Sparsity								
		1	2	4	8	16	32	64	128	256
		Perplexity (↓) for given sparsity								
Tiny	MoSA	22.46	21.76	20.45	19.24	18.00	16.90	**16.39**	17.27	18.06
	Pure MoSA	**22.46**	22.96	23.30	24.78	29.76	-	-	-	-
Small	MoSA	16.01	15.74	15.10	14.48	13.65	12.97	**12.85**	-	-
	Pure MoSA	**16.01**	16.35	17.16	19.61	25.41	-	-	-	-
Med.	MoSA	13.95	13.52	12.81	12.16	11.47	**11.06**	-	-	-
	Pure MoSA	**13.95**	14.03	14.40	15.87	20.63	-	-	-	-
Large	MoSA	12.20	11.33	**10.58**	-	-	-	-	-	-
	Pure MoSA	12.20	**11.83**	11.97	-	-	-	-	-	-
		Number of parameters for given sparsity								
Tiny	MoSA	28M	34M	48M	78M	136M	242M	423M	693M	1B
	Pure MoSA	28M	39M	65M	119M	222M	-	-	-	-
Small	MoSA	113M	127M	163M	229M	360M	599M	1B	-	-
	Pure MoSA	113M	142M	203M	324M	559M	-	-	-	-
Med.	MoSA	210M	239M	310M	442M	703M	1.2B	-	-	-
	Pure MoSA	210M	267M	390M	632M	1.1B	-	-	-	-
Large	MoSA	516M	650M	943M	-	-	-	-	-	-
	Pure MoSA	516M	703M	1B	-	-	-	-	-	-
		Number of MoSA heads for given sparsity								
Tiny	MoSA	0	13	31	69	142	276	505	848	1277
	Pure MoSA	0	23	56	124	255	-	-	-	-
Small	MoSA	0	11	26	54	109	210	381	-	-
	Pure MoSA	0	21	47	98	197	-	-	-	-
Med.	MoSA	0	11	26	54	109	210	-	-	-
	Pure MoSA	0	21	47	98	197	-	-	-	-
Large	MoSA	0	27	60	-	-	-	-	-	-
	Pure MoSA	0	37	80	-	-	-	-	-	-

Table 7: Detailed statistics of the main IsoFLOP experiments from Sec. 3.1. Models Tiny, Small, Medium, and Large are as described in App. G. Sparsity 1 corresponds to dense baselines. Pure MoSA models for sparsities ≥ 1 have only MoSA heads, calculated as the biggest number of heads that will not increase the FLOP budget of the dense baseline (other hyperparameters stay the same as in the baseline). MoSA models have 4 dense heads and the rest of the heads are sparse, calculated such that the FLOP cost of both dense and sparse heads is lower than the baseline. Therefore, the total number of heads in hybrid models (with sparsity ≥ 1) is the number shown in the bottom table + 4. For perplexity, the best result for each row is bold.

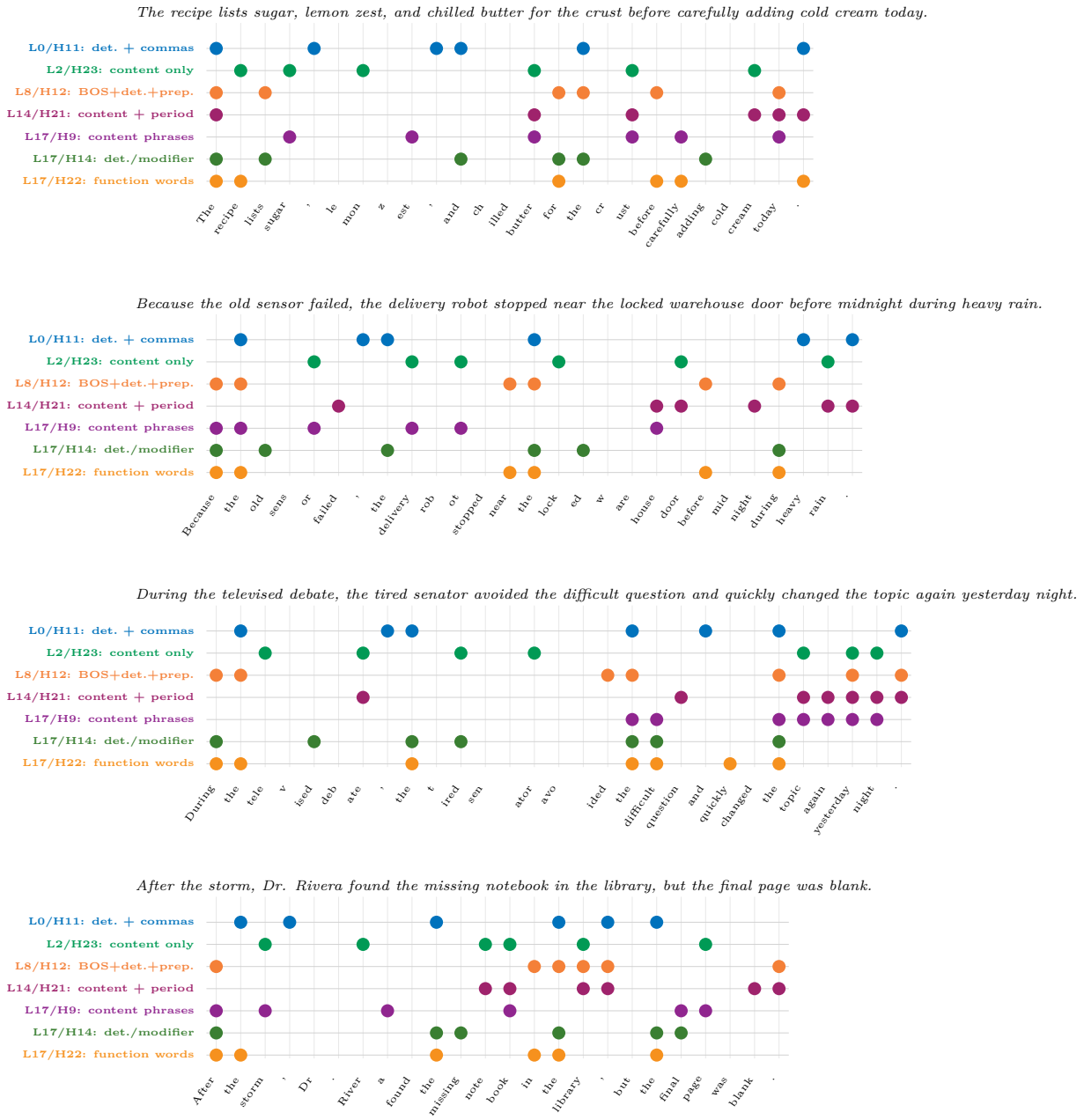

Figure 9: Examples of MoSA routing specialization for seven heads. The first four (L0/H11, L2/H23, L8/H12, L14/H21) are taken from four different layers and illustrate the depth-wise change in routing style. The remaining three (L17/H9, L17/H14, L17/H22) are additional heads from the last layer (17) and illustrate within-layer head diversity. Each panel shows one of four hand-written sentences tokenized into SentencePiece-like fragments; dots mark the tokens selected by the same head across panels. Across depth: the early-layer head (L0/H11) repeatedly fires on the determiner *the* and on commas, the layer-2 head (L2/H23) is a pure content selector with no attention-sink behavior, the mid-layer head (L8/H12) anchors on BOS and on determiner-plus-preposition clusters, and the late-layer head (L14/H21) attends to content tokens near the end of the sentence. Within the last layer: L17/H9 selects content-heavy phrases while skipping most function words, L17/H14 leans toward determiners and modifiers, and L17/H22 emphasizes function words such as determiners and prepositions. These labels summarize recurring tendencies rather than exact symbolic rules.